Supplementary information for

Solvent-free Synthesis of Trisphenols as a Starting Precursor for Synthesis of Calix[4]arenes Using Sulfonated Multi-Walled Carbon Nanotubes

Reza Fareghi-Alamdari*; Mohsen Golestanzadeh; Negar Zekri

College of Chemistry and Chemical Engineering, Malek-Ashtar University of Technology, Tehran, 16765-3454, I. R. Iran

Email: reza_fareghi@yahoo.com, mohsengolestanzadeh@yahoo.com

Tel: +982122970277, Fax: +982122970195

Contents:

Microscopic and spectroscopic characterization of prepared catalyst

The SO_3H@MWCNTs catalyst was characterized by the following techniques: Scanning Electron Microscopy (SEM) (Fig. S1a and S1b); Transmission Electron Microscopy (TEM) (Fig. S1c and S1d); FT-IR spectroscopy (Fig. S2); Powder X-ray Diffraction (XRD) (Fig. S3); Raman Spectroscopy (Fig. S4); and Thermal Gravimetric Analysis (TGA) (Fig. S5).

SEM and TEM results

SEM images of MWCNTs and SO_3H@MWCNTs are shown in Figure S1a and S1b respectively. The SEM images revealed that after applied strategy for functionalization of MWCNTs the tubular structure of CNTs are still tube-shape and they did not destroy in this process. Also, Figure S1b shows that the morphology of the surface after functionalization was changed. The TEM images of MWCNTs and SO_3H@MWCNTs at scale bar 160 and 16 nm are shown in Figure S1c and S1d respectively. In these Figures the tubular structure of CNTs were seen and the results of SEM images were confirmed. Also, compared with the raw MWCNTs the prepared catalyst was covered by a foreign material.

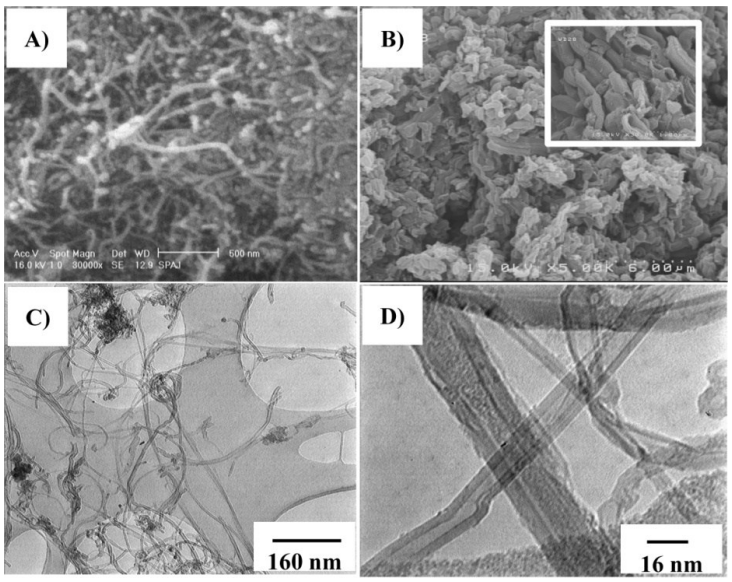

Figure S1, SEM images of (A): MWCNTs (B): SO_3H@MWCNTs; TEM images of (C): MWCNTs (D): SO_3H@MWCNTs

FT-IR spectroscopy

Figure S2 shows the FT-IR spectra of MWCNTs, COOH@MWCNTs, and SO_3H@MWCNTs. Comparison between the FT-IR spectra of raw MWCNTs, COOH@MWCNTs, and SO_3H@MWCNTs reveals some absorption bonds in the COOH@MWCNTs, and SO_3H@MWCNTs that are not present in the raw MWCNTs. In accordance with spectrum (A), the peak at ~3300 cm^{-1} is related to the presence of water in KBr pellet. In COOH@MWCNTs due to the changed the symmetry of CNTs, the absorbance bonds are related to the C-O stretching, C=O stretching, O-H stretching, and C-O-C bending vibration. Also, distinguished peaks at 3346, 1624, 1512, and 1150 cm^{-1} confirmed the presence of hydroxyl on carboxylic acid on the surface of MWCNTs. In addition, in spectrum (C) the peaks positioned at 1278, 1109, and 553 cm^{-1} are associated to the stretching symmetry and asymmetry of the S=O bond and C-S respectively.

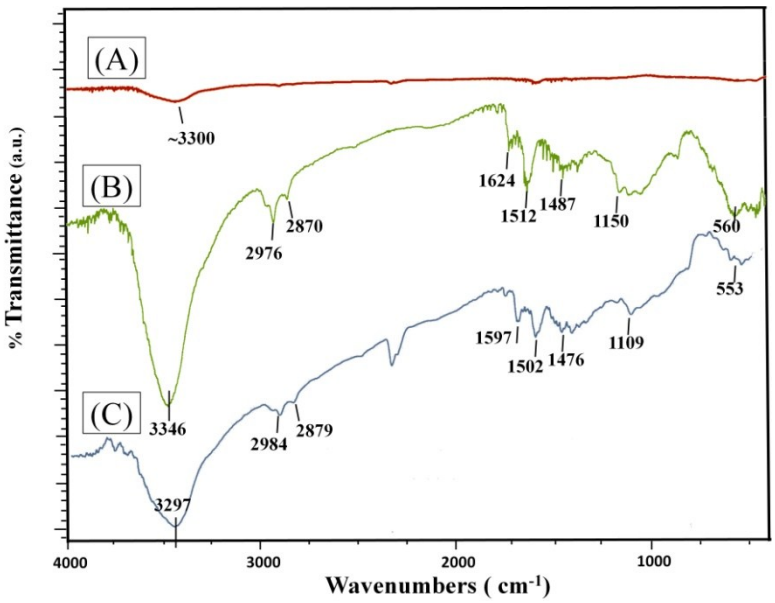

Figure S2, Comparison between the FT-IR spectra of (A): MWCNTs (B): COOH@MWCNTs (C): SO_3H@MWCNTs

XRD results

Figure S3 shows the XRD pattern of SO_3H@MWCNTs after functionalization. This pattern displays that the crystal structure of CNTs are still tubular relative to the XRD pattern of raw CNTs. Two peaks are indexed as the (001) and (112) planes of the CNTs at 2θ: 27.3 and 41° respectively.

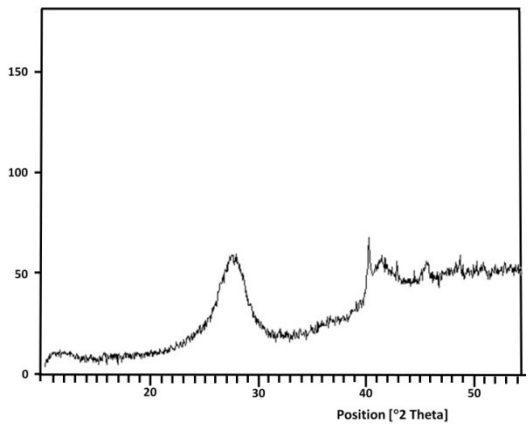

Figure S3, XRD pattern of SO_3H@MWCNTs

Raman spectroscopy

Figure S4, shows the Raman spectra of MWCNTs, COOH@MWCNTs and SO_3H@MWCNTs. As shown in this Figure, the spectrum exhibit three peaks at about 1320, 1571 and 2660 cm^{-1}. The peak at 1571 cm^{-1} is determined with the tangential mode (G-band). The origin of the line at 1320 cm^{-1} is the D-band and its appearance has been tentatively assigned to a symmetry lowering effect, such as the presence of nanoparticles (synthesis of CNTs) and functional groups such as sulfonic acid on the side walls of MWCNTs. The line at 2660 cm^{-1} has been attributed to the overtone of the D-band (G′-band). We can calculate that I_D/I_G values of MWCNTs, COOH@MWCNTs and SO_3H@MWCNTs are 0.24, 0.37 and 0.84, respectively. This increasing value implies that a strong damage to the side walls of CNTs is due to the functionalization. The existence of RBM in low frequency of SO_3H@MWCNTs indicated that MWCNTs are still in their tubular structure after treatment of sulfuric acid and functionalization, although some MWCNTs were probably damaged by strong oxidation.

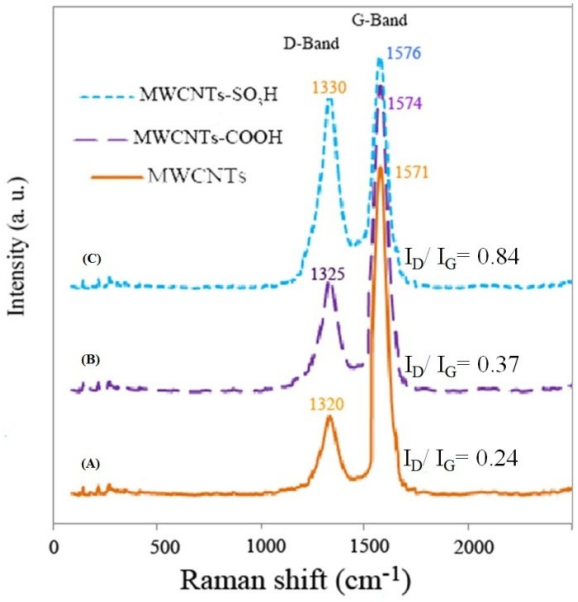

Figure S4, Raman spectra of (A): MWCNTs (B): COOH@MWCNTs (C): SO_3H@MWCNTs

TGA results

TGA thermograms were used to determine the amount of formed sulfonic and carboxylic acid groups onthe side wall of the MWCNTs. Figure S5 show thermograms of COOH@MWCNTs, and SO_3H@MWCNTs. The weight loss between 100 °C and 200 °C is entirely due to the presence of amorphous carbon, water, metals and so on. Also, the weight loss between 200 °C and 600 °C is completely due to functional groups on the end and side wall of the MWCNTs. It is possible that these functional groups in this research are OH, COOH, and SO_3H groups. As shown in Figure S5a, the attached COOH group decomposed at about ~250 °C and 18% weight was decreased. After treatment of the H_2SO_4 with COOH@MWCNTs, TGA of the SO_3H@MWCNTs showed the 49% weight was deleted. Accordingly these results indicate that 67% weight can be ascribed to the covalently of sulfonic and carboxylic acid groups to the side wall of the MWCNTs. Taking into account that the covalently SO_3H measurements indicated one functionality every ~five C atoms in the MWCNTs-SO_3H. Results obtained by TGA thermograms showed good agreement with results of FT-IR spectroscopy and Raman spectroscopy.

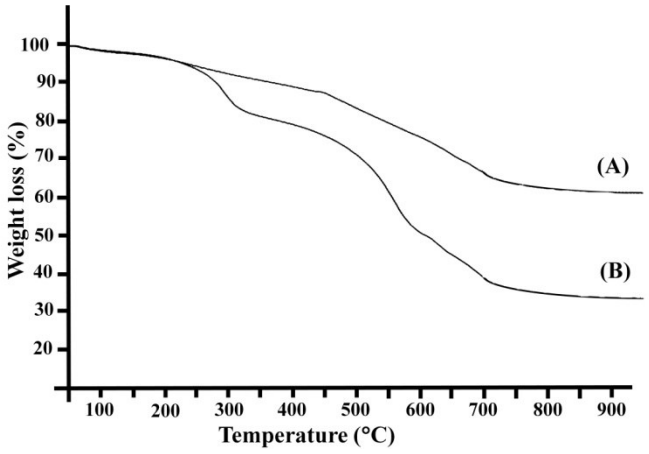

Figure S5, TGA curve of (A): COOH@MWCNTs (B): SO_3H@MWCNTs

For calculation the extent of functionalization per C atoms, weight loss values were employed together with the molecular weight of the different groups and the following Equation was applied. Where X stands for the number of carbon atoms in the CNTs sample per each covalent functional group, R (%) is the residual mass at 600 °C in the TGA plot, L (%) is the weight loss in the range of 200°C and 600 °C, and Mw is the molecular weight of the desorbed functional groups.

$$\text{Equation(1): } X = \frac{R\,(\%) \times Mw\left(\frac{g}{mol}\right)}{L\,(\%) \times 12\left(\frac{g}{mol}\right)}$$

Acidity measurement of the catalysts

Acid-base titration was employed to determine the density of sulfonic acid groups on the side wall of the SO_3H@MWCNTs. The volume required to reach the neutral point was subtracted from the initial volume of NaOH used to obtain the volume of NaOH which has reacted with SO_3H group on the side wall MWCNTs (Equation 3). The measurement was repeated three times for each sample and the average calculated. The acid-base titration showed that the amount of SO_3H attached to MWCNTs is 1.80 $mmol.g^{-1}$. In addition, after preparation of COOH@MWCNTs, we calculate amount of –OH and –COOH by acid-base titration as described above. Acid-base titration for MWCNTs-COOH was 0.15 $mmol.g^{-1}$.

(Equation 2)

NaOH (mmol reacted with SO_3H) = NaOH (primary mmol) - NaOH (mmol unreacted with SO_3H)

Copy of ^{1}H NMR and ^{13}C NMR of synthetic compounds

2,6-Bis-(2-hydroxybenzyl)-phenol (Compound C1)

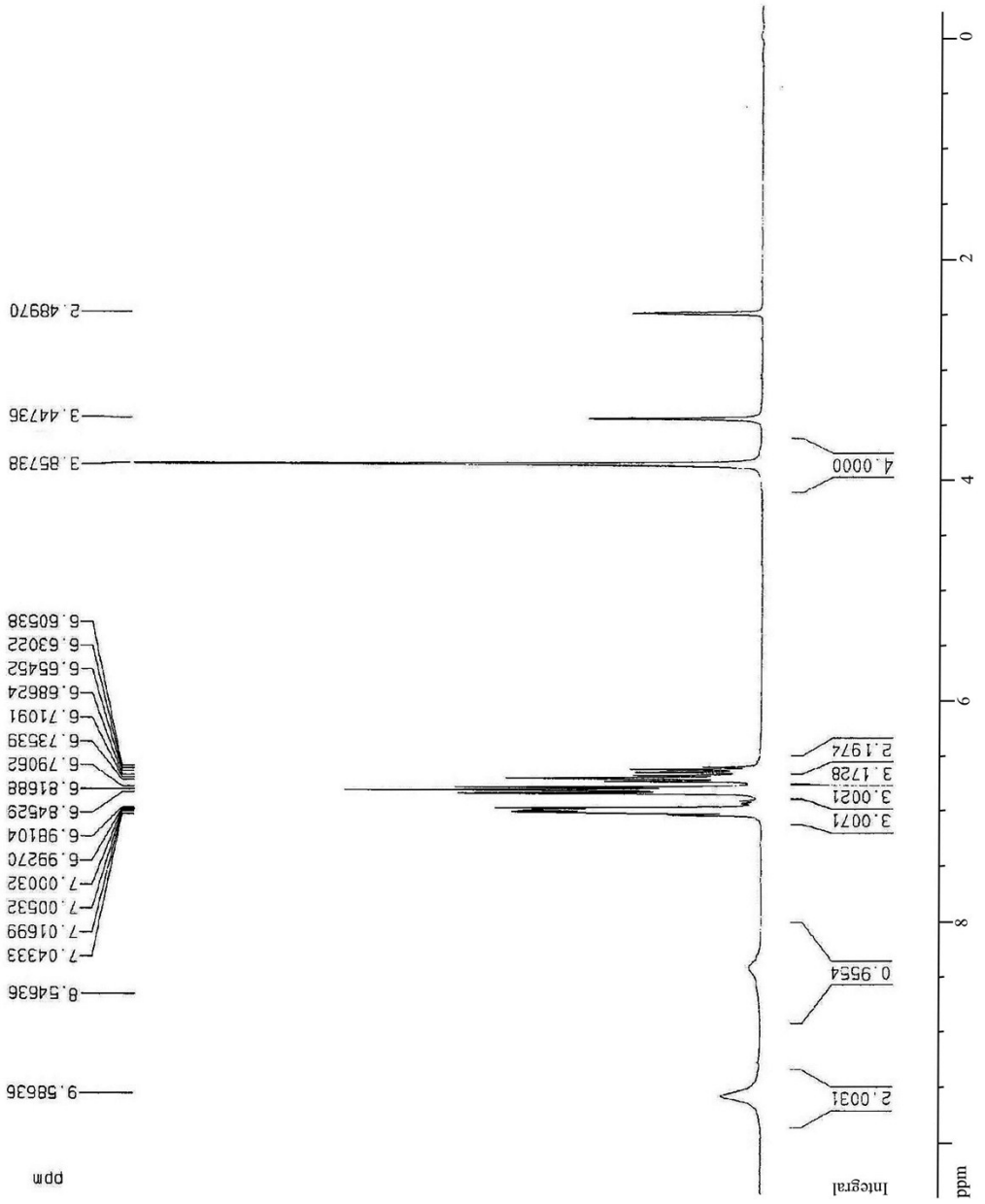

ppm
0
50
100
150
200
29.820
38.665
38.943
39.221
39.499
39.777
40.055
40.333
114.863
119.159
119.371
126.897
127.022
127.584
127.849
130.319
152.354
154.694

2,6-Bis-(2-hydroxy-5-methylbenzyl)-4-methylphenol (Compound C2)

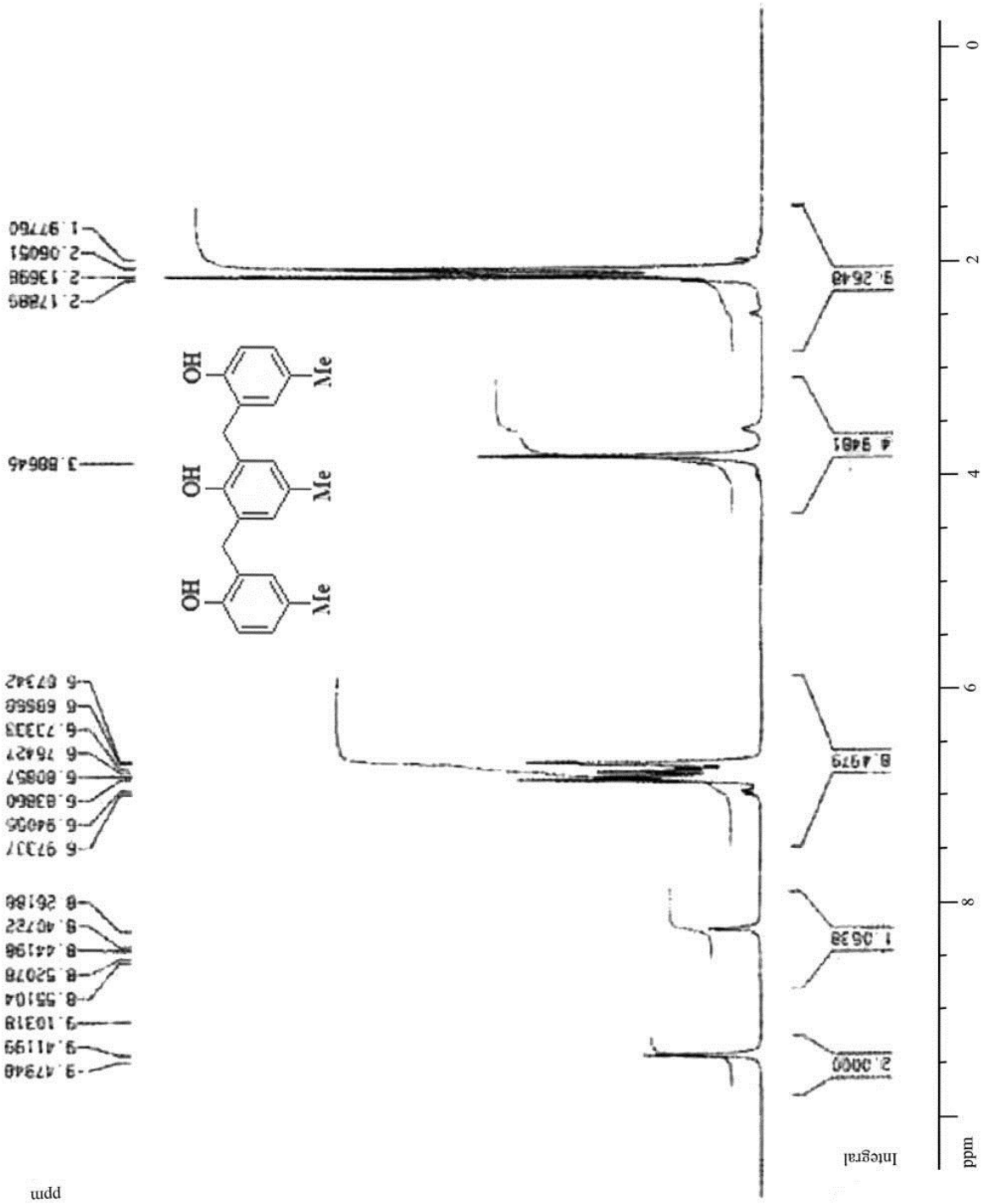

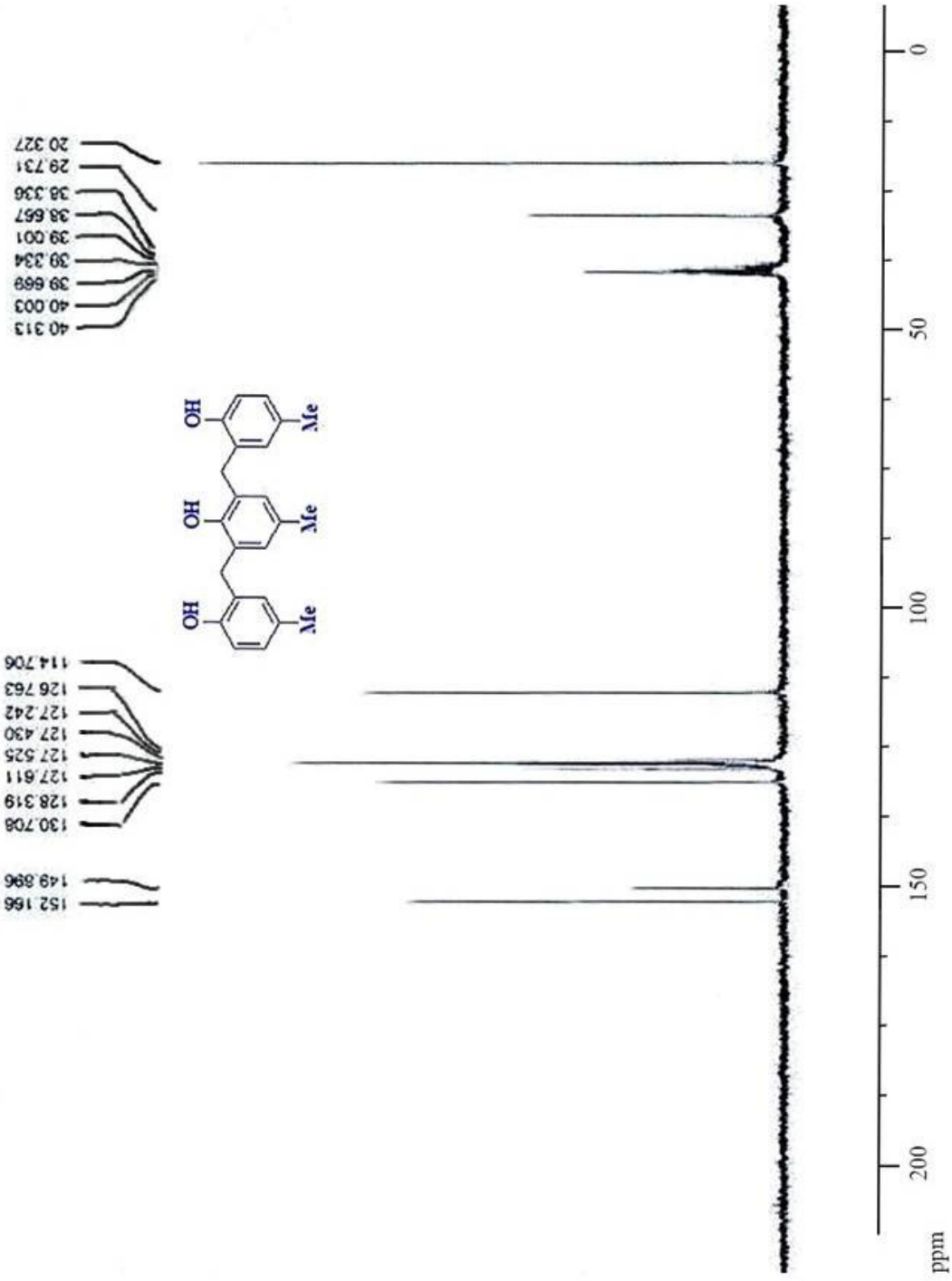
20.327
29.731
38.336
38.667
39.001
39.334
39.668
40.003
40.313
OH
Me
OH
Me
OH
Me
114.706
126.763
127.242
127.430
127.525
127.611
128.319
130.708
149.896
152.166
0
50
100
150
200
ppm

2,6-Bis-(2-hydroxy-5-methyl-3-*tert*-butylbenzyl)-4-methylphenol (Compound C3)

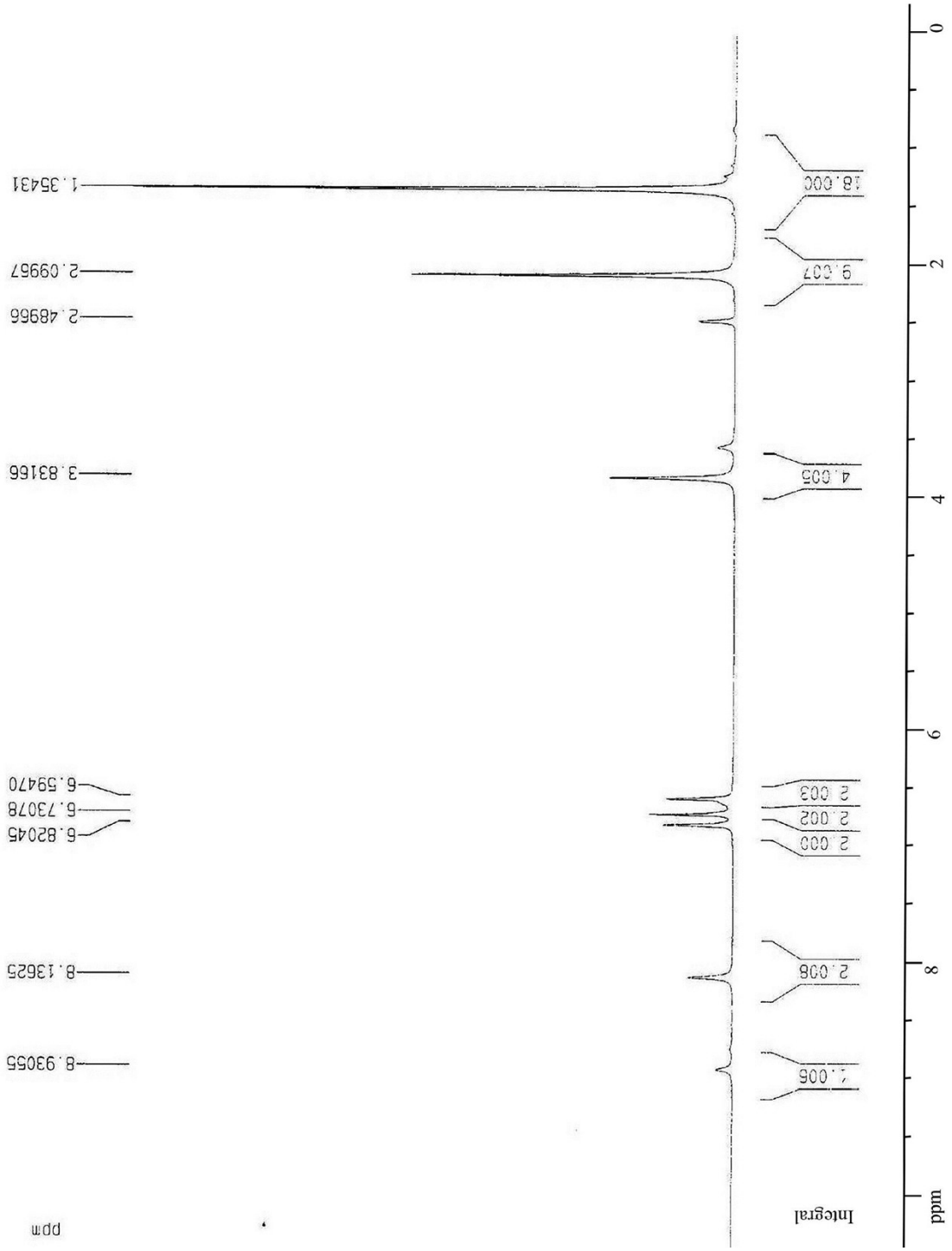

20.374
20.748
29.834
30.524
34.413
38.696
38.973
39.251
39.529
39.807
40.085
40.362
124.968
127.611
127.657
127.883
128.531
128.733
129.119
136.789
149.260
150.545
ppm
0
50
100
150
200
ppm

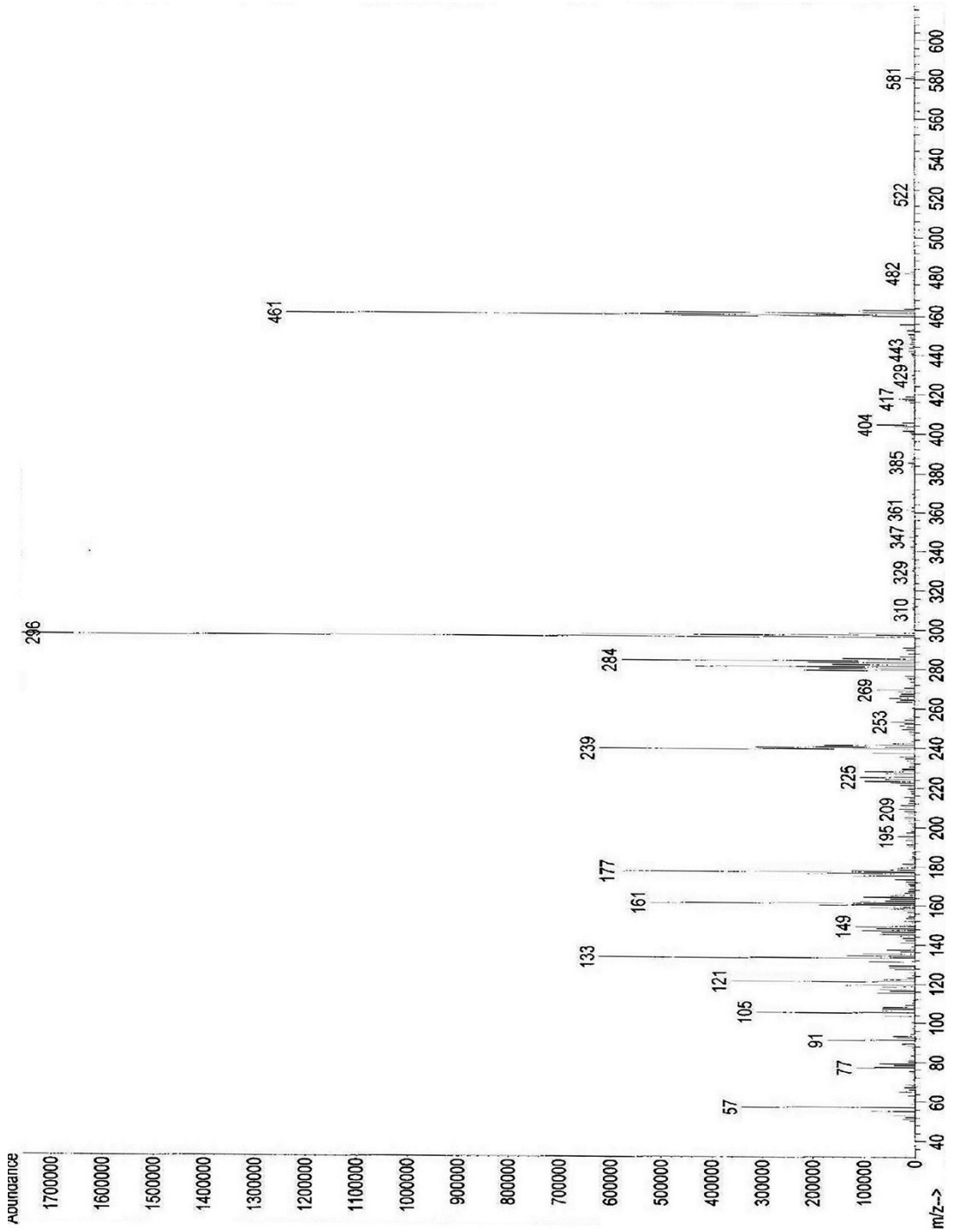
Abundance
m/z-->

2,6-Bis-(5-Bromo-2-hydroxybenzyl)-4-methylphenol (Compound C4)

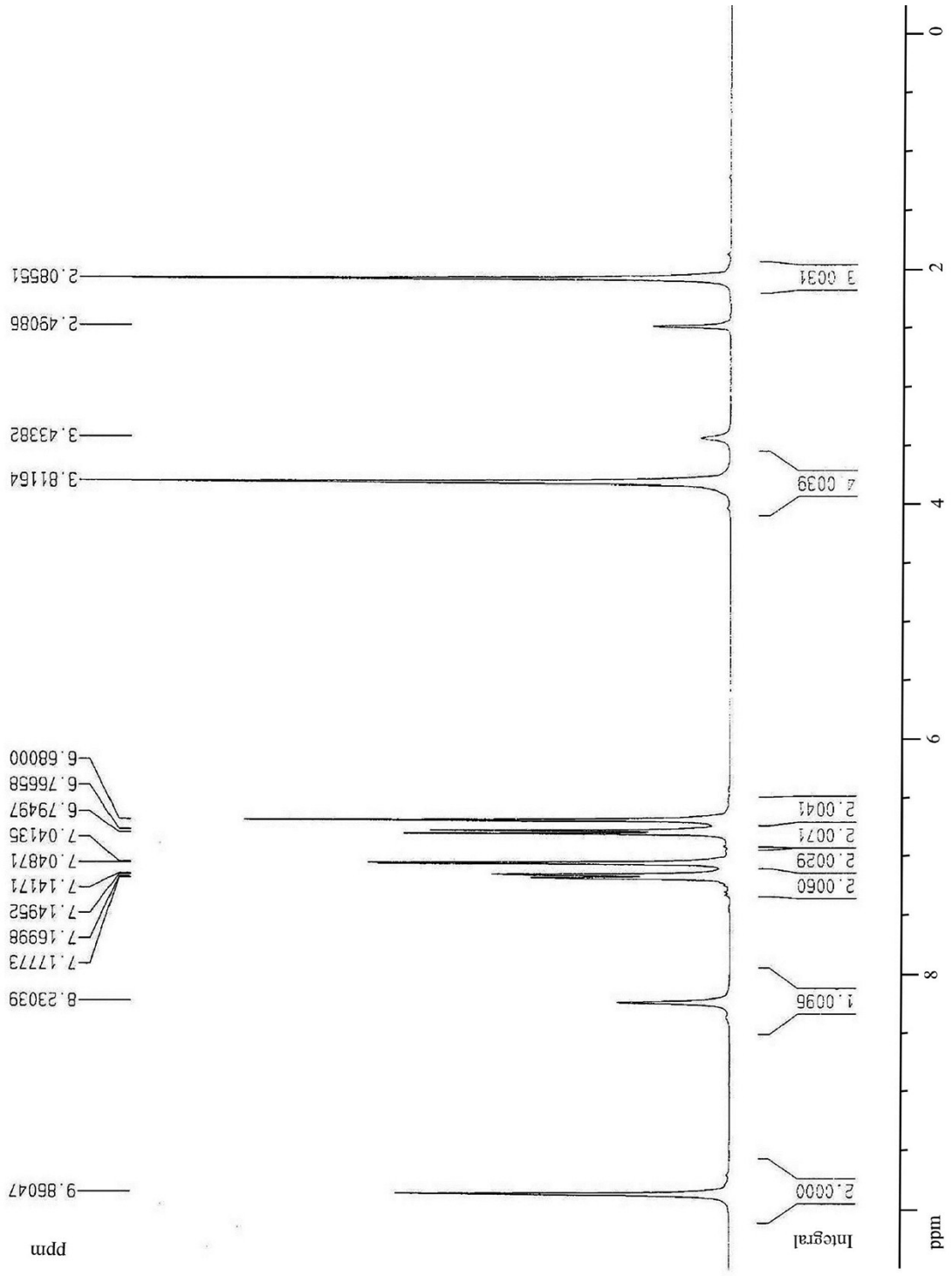

ppm
0
50
100
150
200
20.380
29.581
38.675
38.952
39.230
39.508
39.786
40.064
40.342
110.150
116.889
126.973
128.016
128.907
129.455
130.111
132.155
150.256
154.264

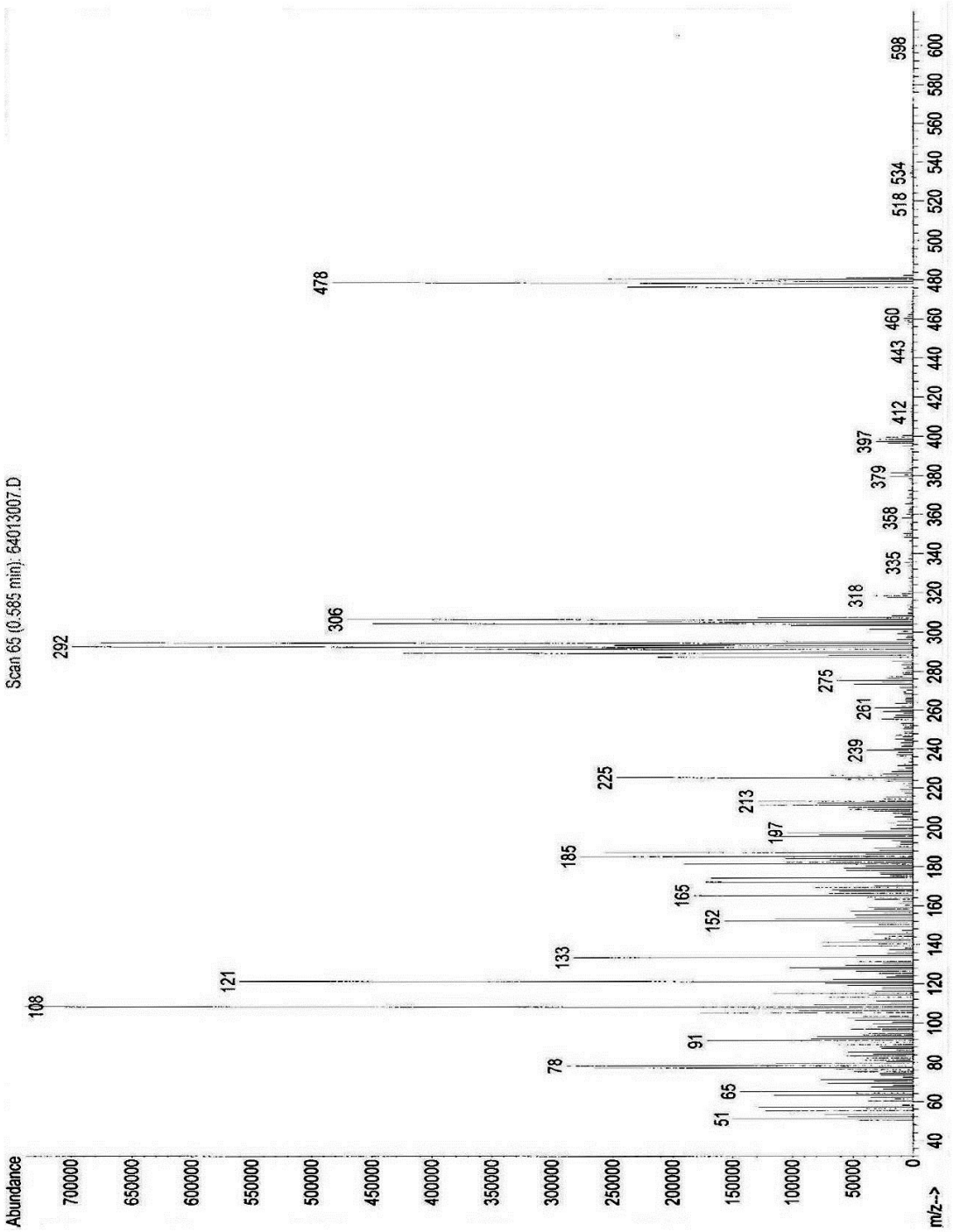
Scan 65 (0.585 min): 64013007.D
Abundance
m/z-->
108
121
133
78
91
65
51
152
165
185
197
213
225
239
261
275
292
306
318
335
358
379
397
412
443
460
478
518
534
598

2,6-bis-(5-chloro-2-hydroxybenzyl)-4-bromophenol (Compound C5)

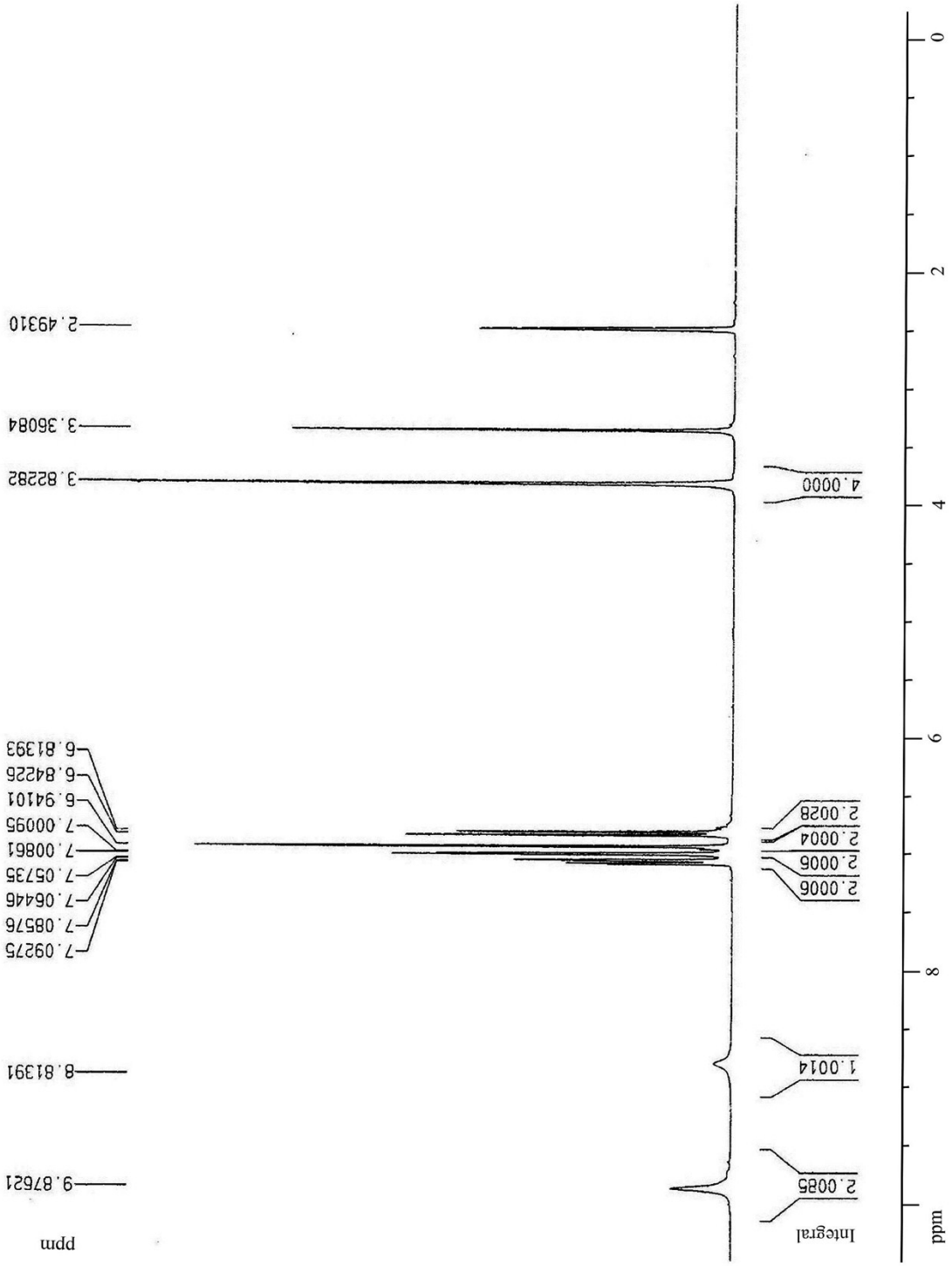

29.542
38.664
38.941
39.219
39.497
39.775
40.053
40.330
110.782
116.422
122.427
126.959
128.390
129.577
129.990
130.113
151.937
153.891
ppm
0
50
100
150
200
ppm

2,6-Bis-(5-chloro-2-hydroxybenzyl)-4-fluorophenol (Compound C6)

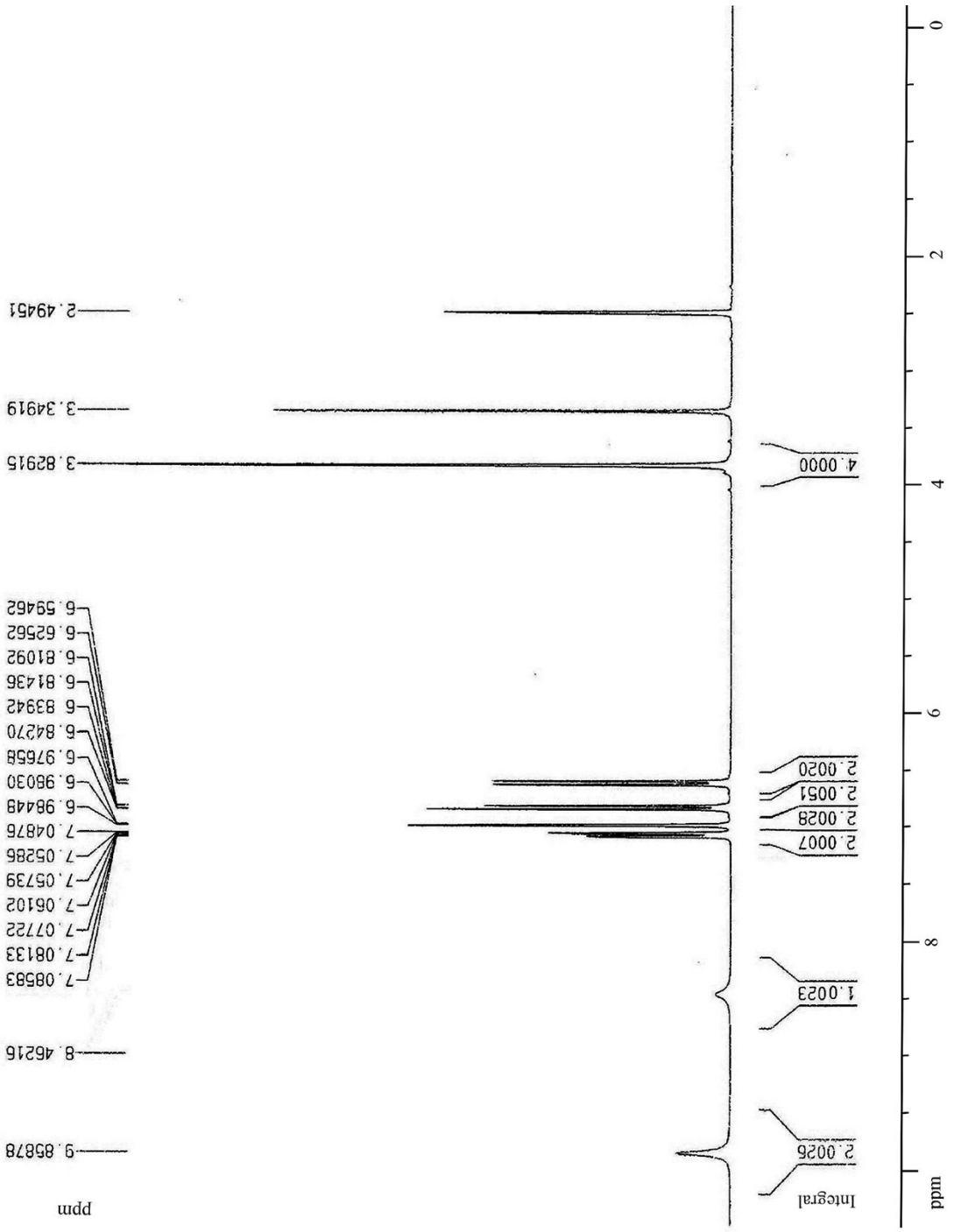

29.772
38.673
38.951
39.229
39.507
39.785
40.063
40.340
113.732
114.031
116.376
122.421
126.873
128.328
128.537
129.109
129.209
129.501
153.883
154.022
157.131
ppm
0
50
100
150
200
ppm

2,6-Bis-(5-chloro-2-hydroxybenzyl)-4-chlorophenol (Compound C7)

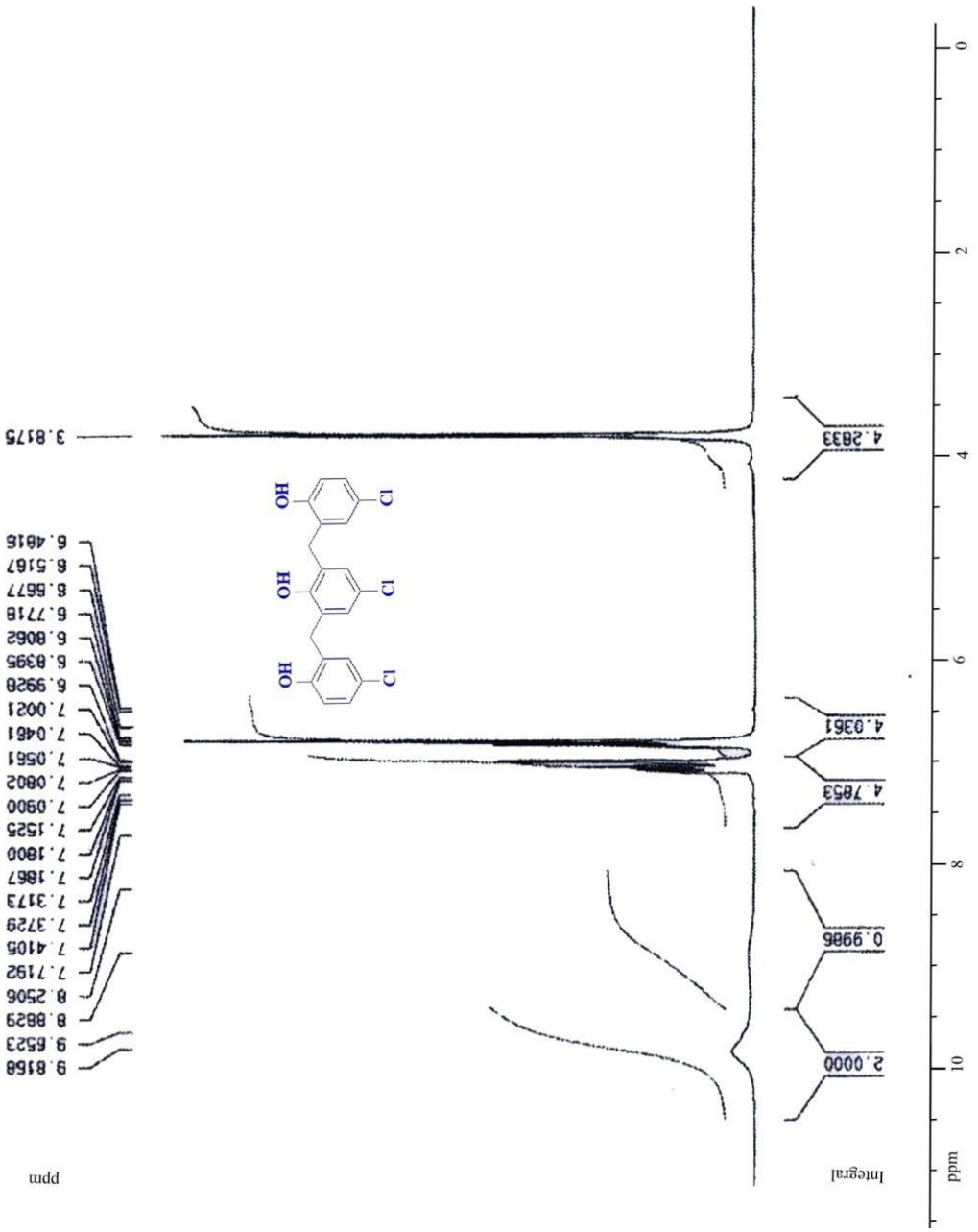

ppm
0
25
50
75
100
125
150
175
153.063
151.413
128.356
127.189
126.874
122.843
122.382
116.380
40.377
40.055
39.719
39.387
39.052
38.719
38.380
29.587
OH
Cl
OH
Cl
OH
Cl

2,6-Bis-(2-hydroxy-5-methylbenzyl)-4-chlorophenol (Compound C8)

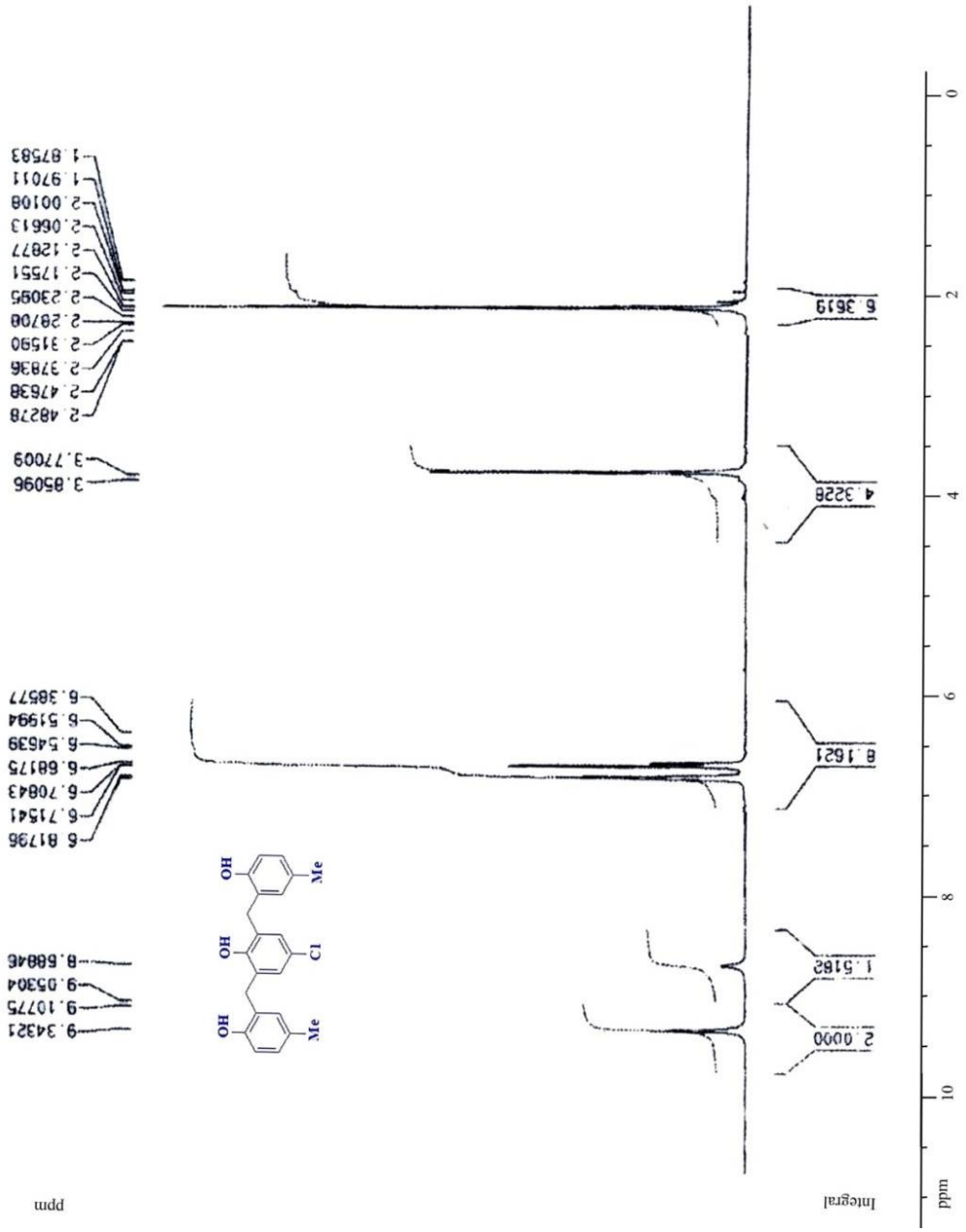

ppm
0
20
40
60
80
100
120
140
160
OH
Me
OH
Cl
OH
Me

2,6-Bis-(5-fluoro-2-hydroxybenzyl)-4-chlorophenol (Compound C9)

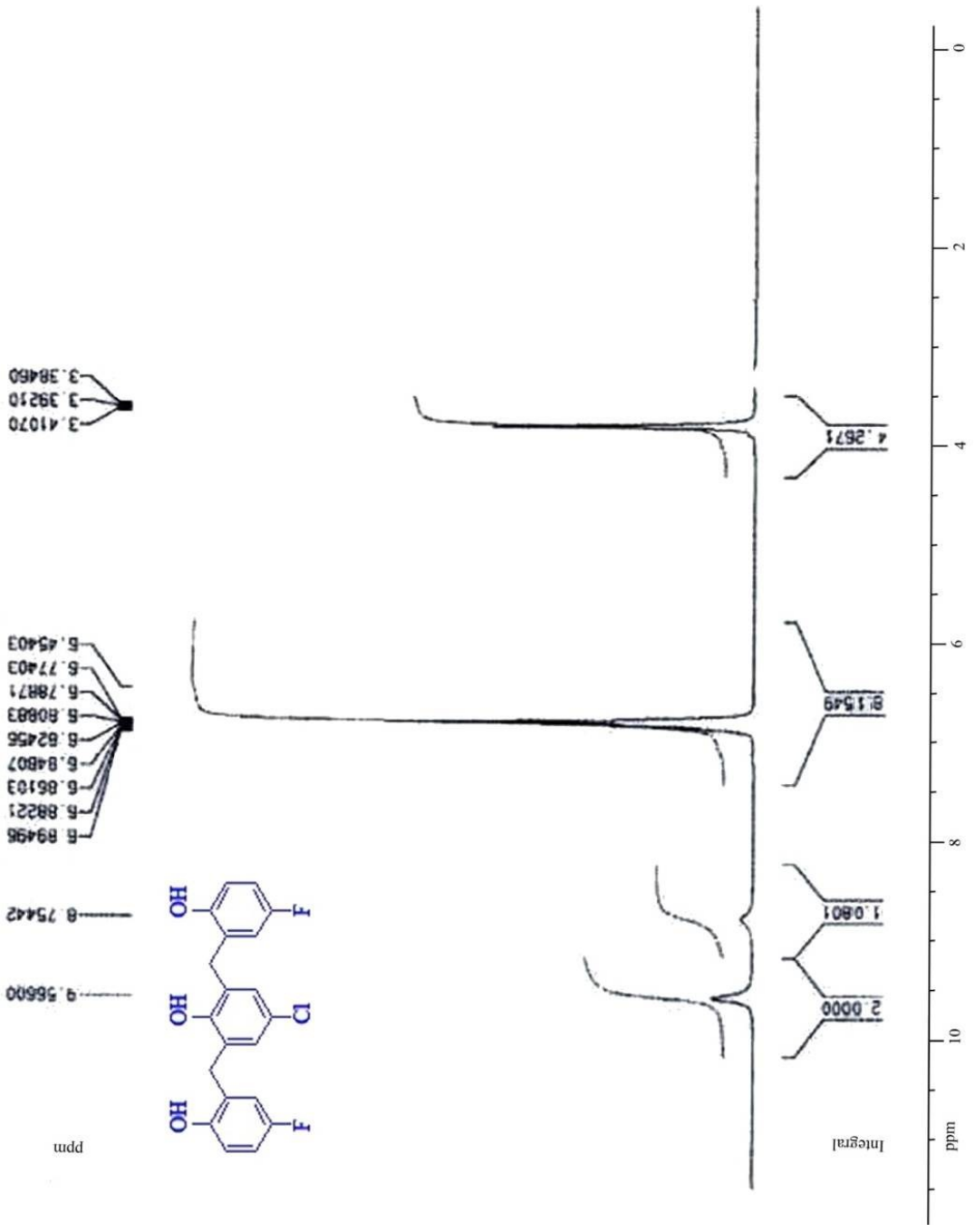

ppm
0
20
40
60
80
100
120
140
160
ppm
OH
F
OH
Cl
OH
F
23.754
38.386
38.720
39.056
39.391
39.725
40.057
40.364
113.060
113.416
115.467
115.596
116.124
116.488
122.858
127.065
127.653
127.768
129.520
151.060
151.351
153.835
157.251

2,6-Bis-(5-bromo-2-hydroxybenzyl)-4-bromophenol (Compound C10)

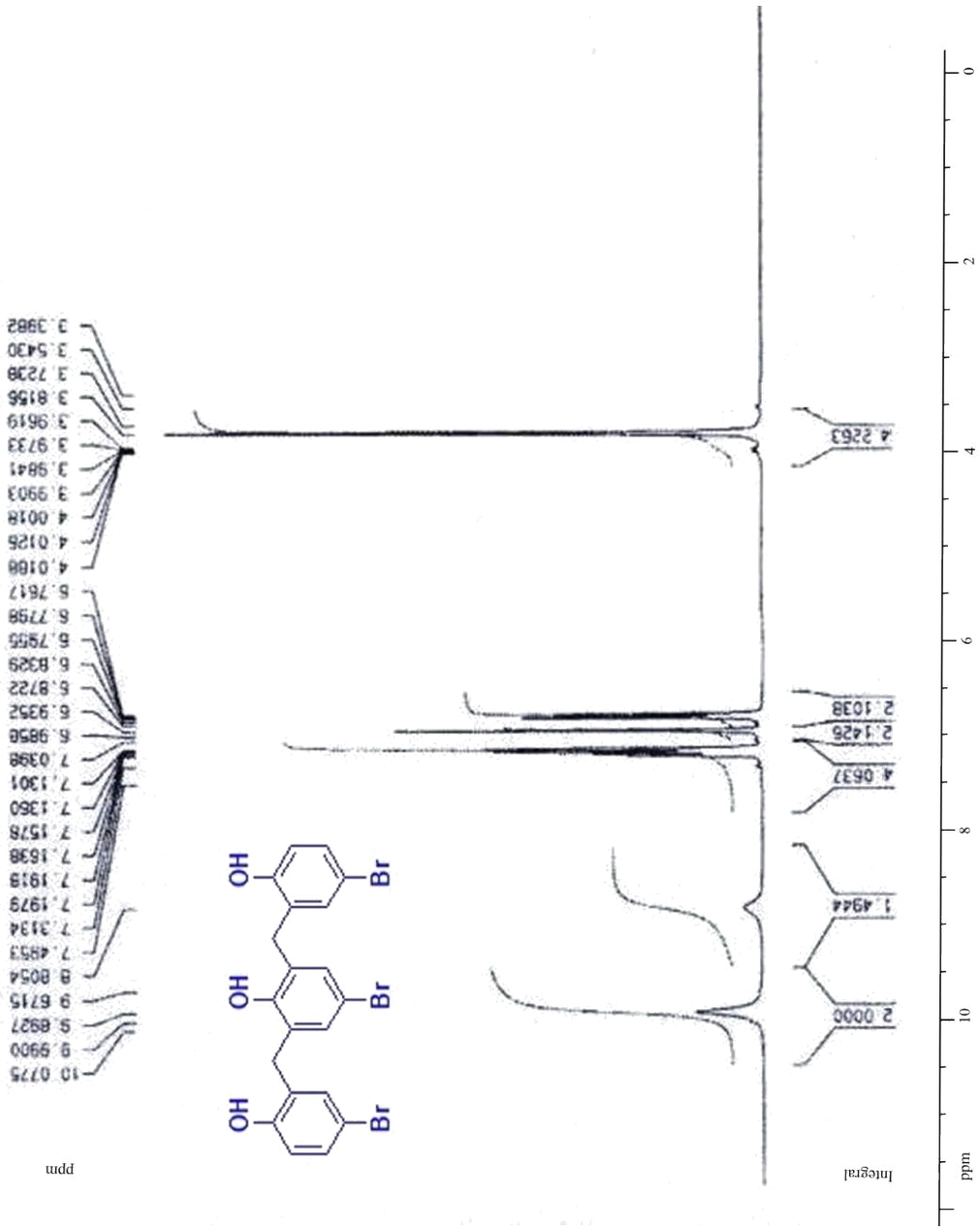

ppm
0
25
50
75
100
125
150
175
OH
Br
OH
Br
OH
Br
40.495
40.094
39.751
39.416
39.084
38.750
38.417
29.435
110.055
110.701
116.986
128.928
129.816
129.951
130.039
132.359
151.851
154.308

2,6-Bis-(5-bromo-2-hydroxybenzyl)-4-chlorophenol (Compound C11)

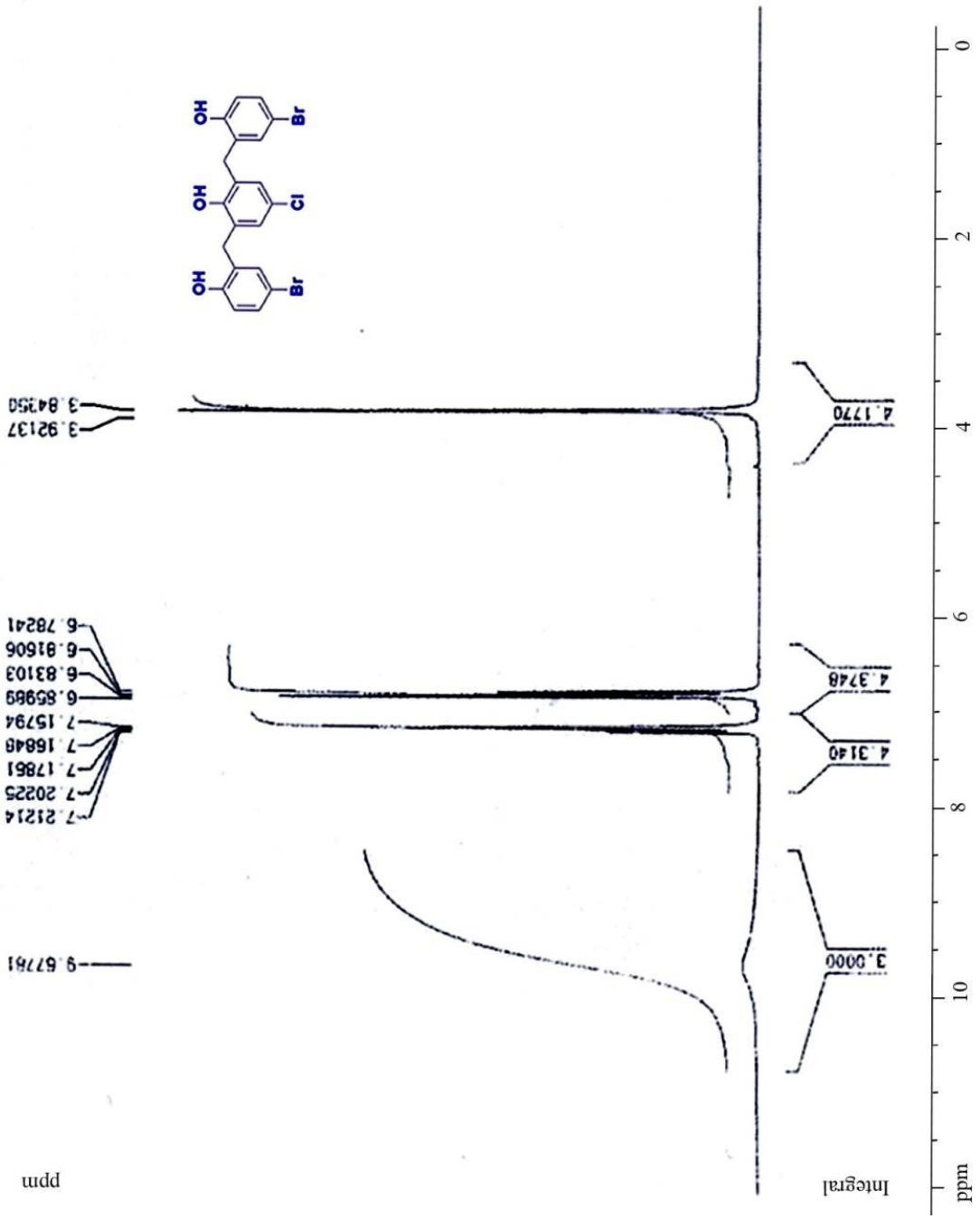

ppm
0
20
40
60
80
100
120
140
160
OH
Br
OH
Cl
OH
Br
29.576
38.348
38.685
39.018
39.352
39.686
40.019
40.346
110.127
116.974
122.879
127.216
128.937
129.431
129.812
132.399
151.371
154.307

2,6-Bis-(5-fluoro-2-hydroxybenzyl)-4-fluorophenol (Compound C12)

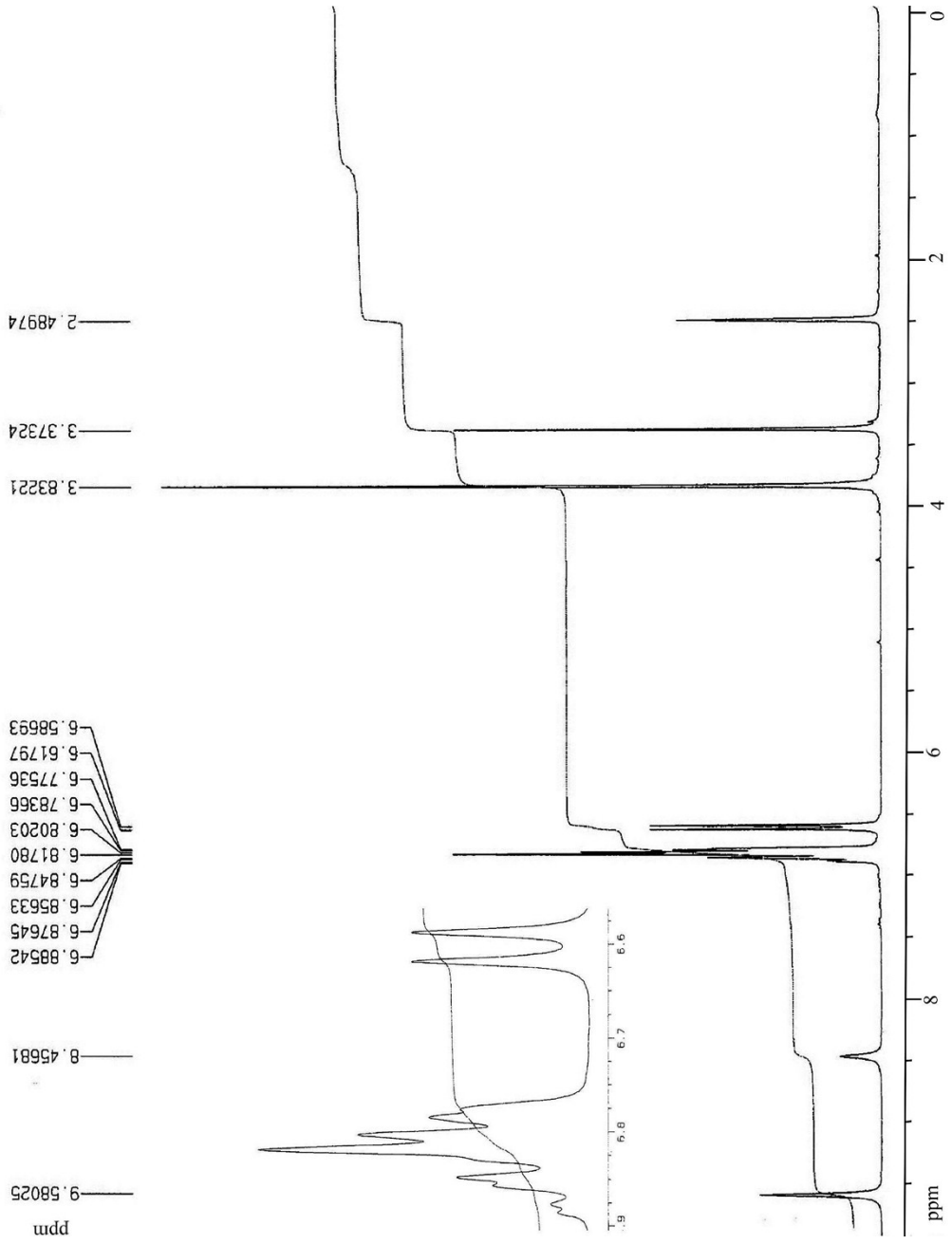

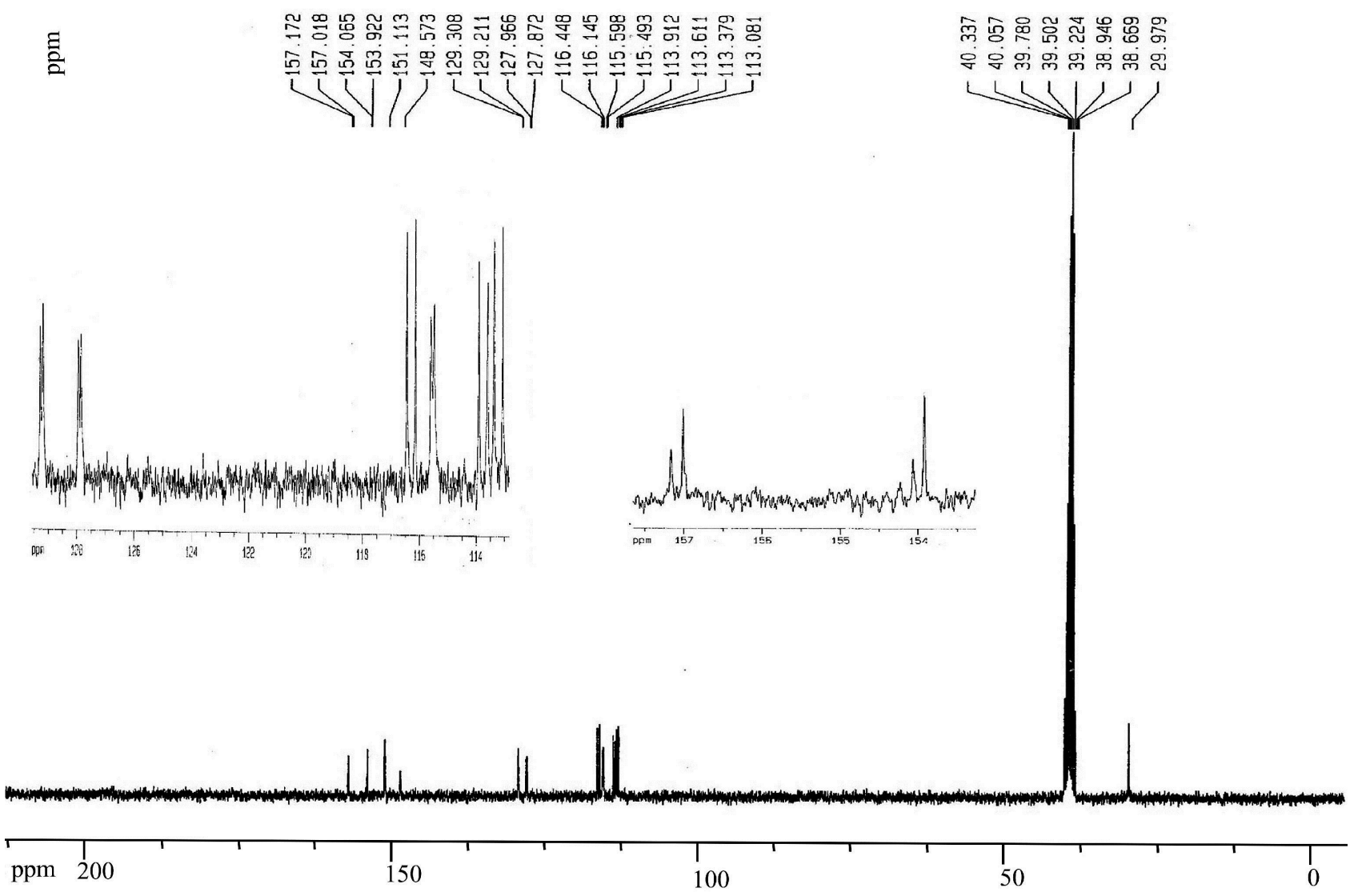
ppm
157.172
157.018
154.065
153.922
151.113
148.573
129.308
129.211
127.966
127.872
116.448
116.145
115.598
115.493
113.912
113.611
113.379
113.081
40.337
40.057
39.780
39.502
39.224
38.946
38.669
29.979
ppm 200
150
100
50
0

2,6-Bis-(5-chloro-2-hydroxybenzyl)-4-methylphenol (Compound C13)

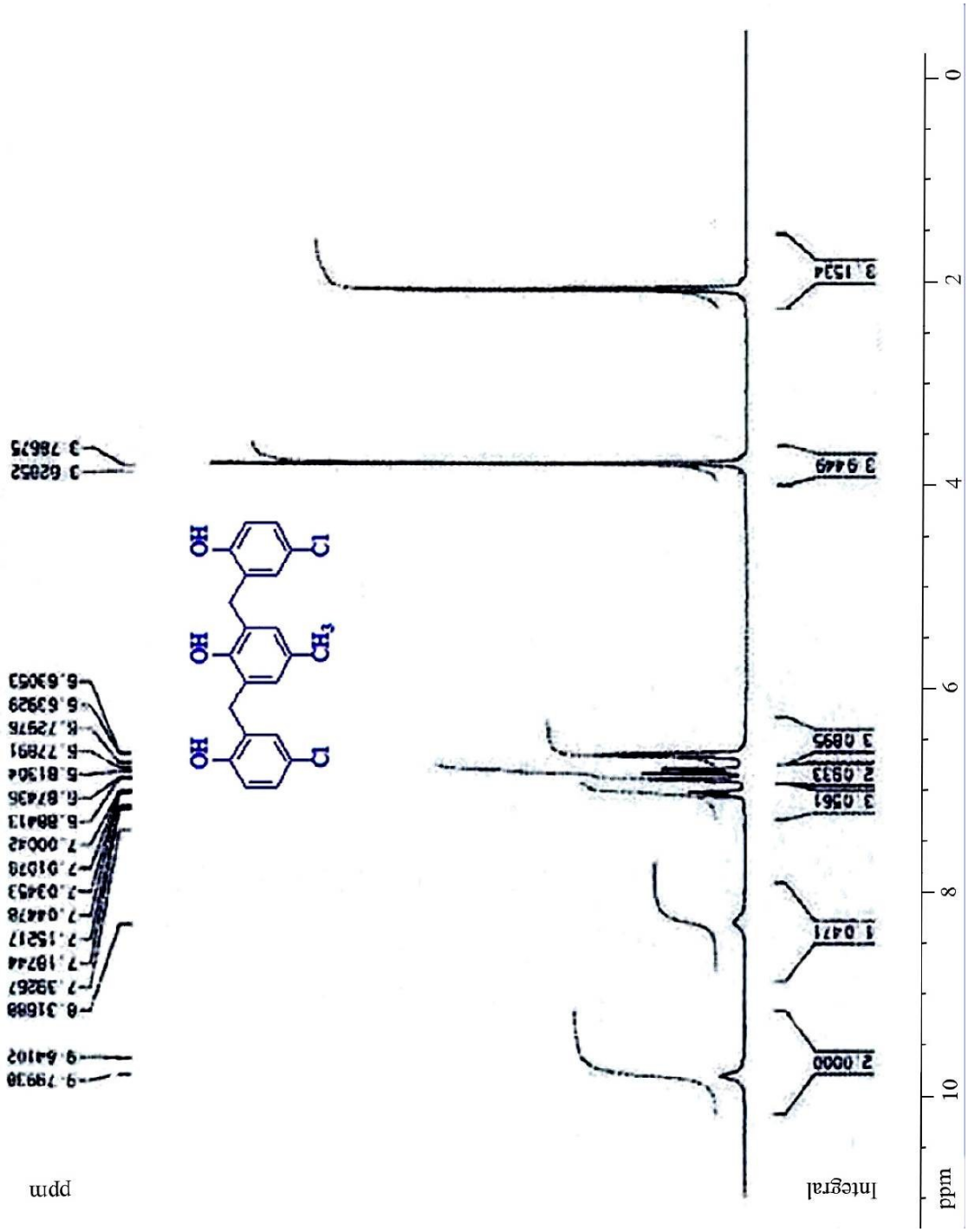

ppm
0
20
40
60
80
100
120
140
160
OH
Cl
OH
CH3
OH
Cl

2,6-Bis-(2,5-dihydroxybenzyl)-4-chlorophenol (Compound C14)

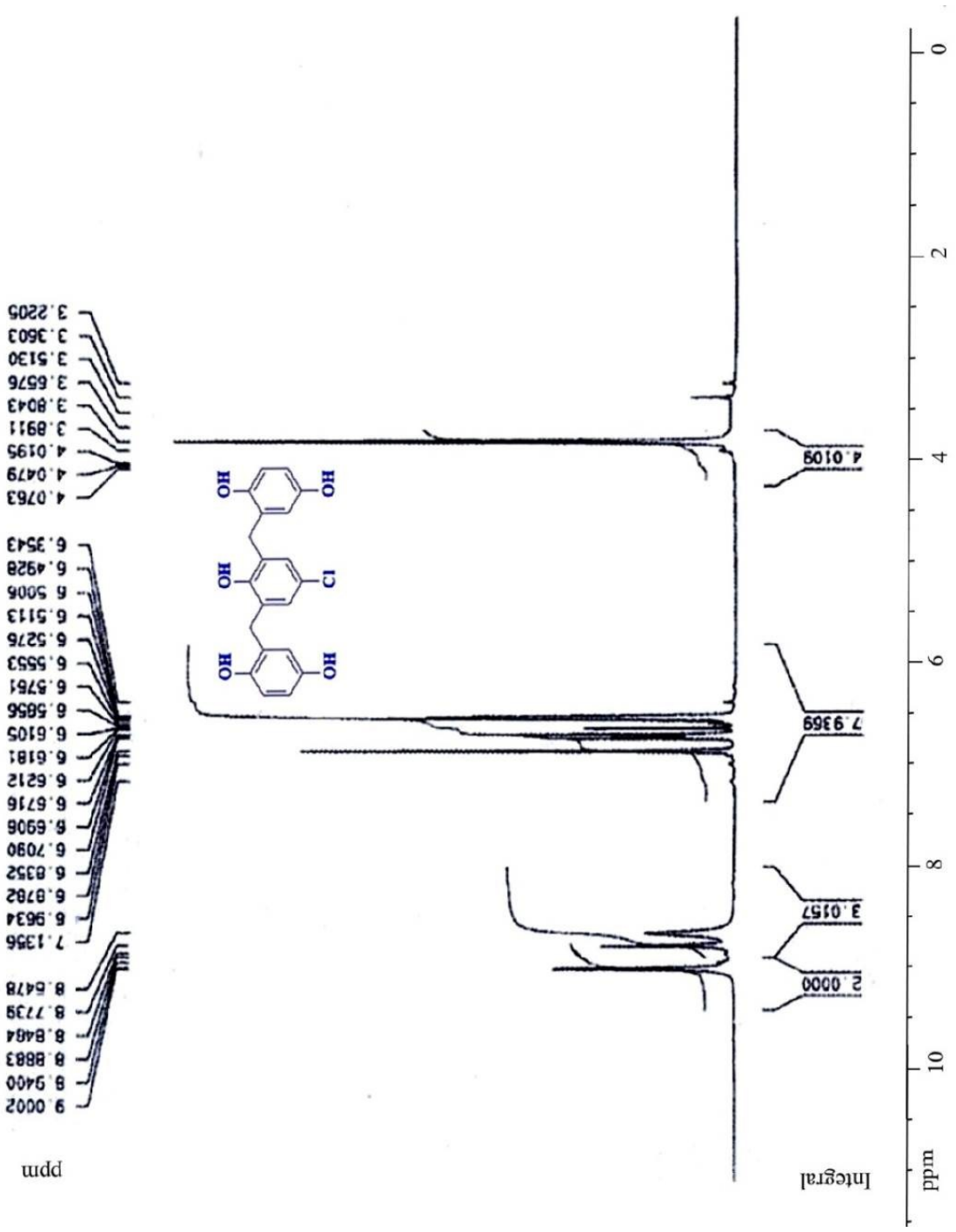

ppm
0
25
50
75
100
125
150
175
OH
OH
OH
Cl
OH
OH

2,6-Bis-(2-hydroxy-5-nitrobenzyl)-4-chlorophenol (Compound C15)

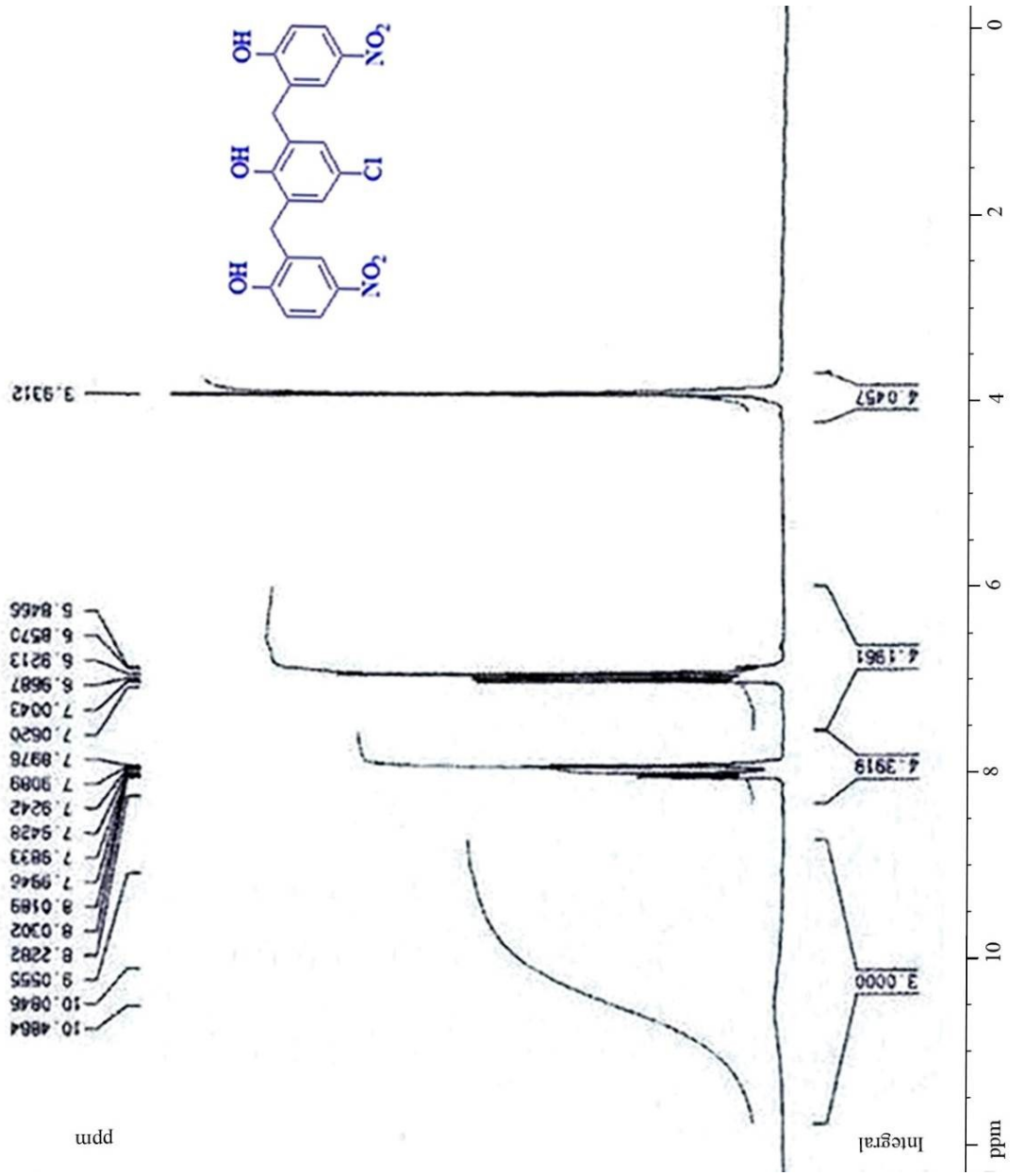

ppm
0
25
50
75
100
125
150
175
OH
NO2
OH
Cl
OH
NO2

2,6-Bis-(2-hydroxy-5-phenylbenzyl)-4-chlorophenol (Compound C16)

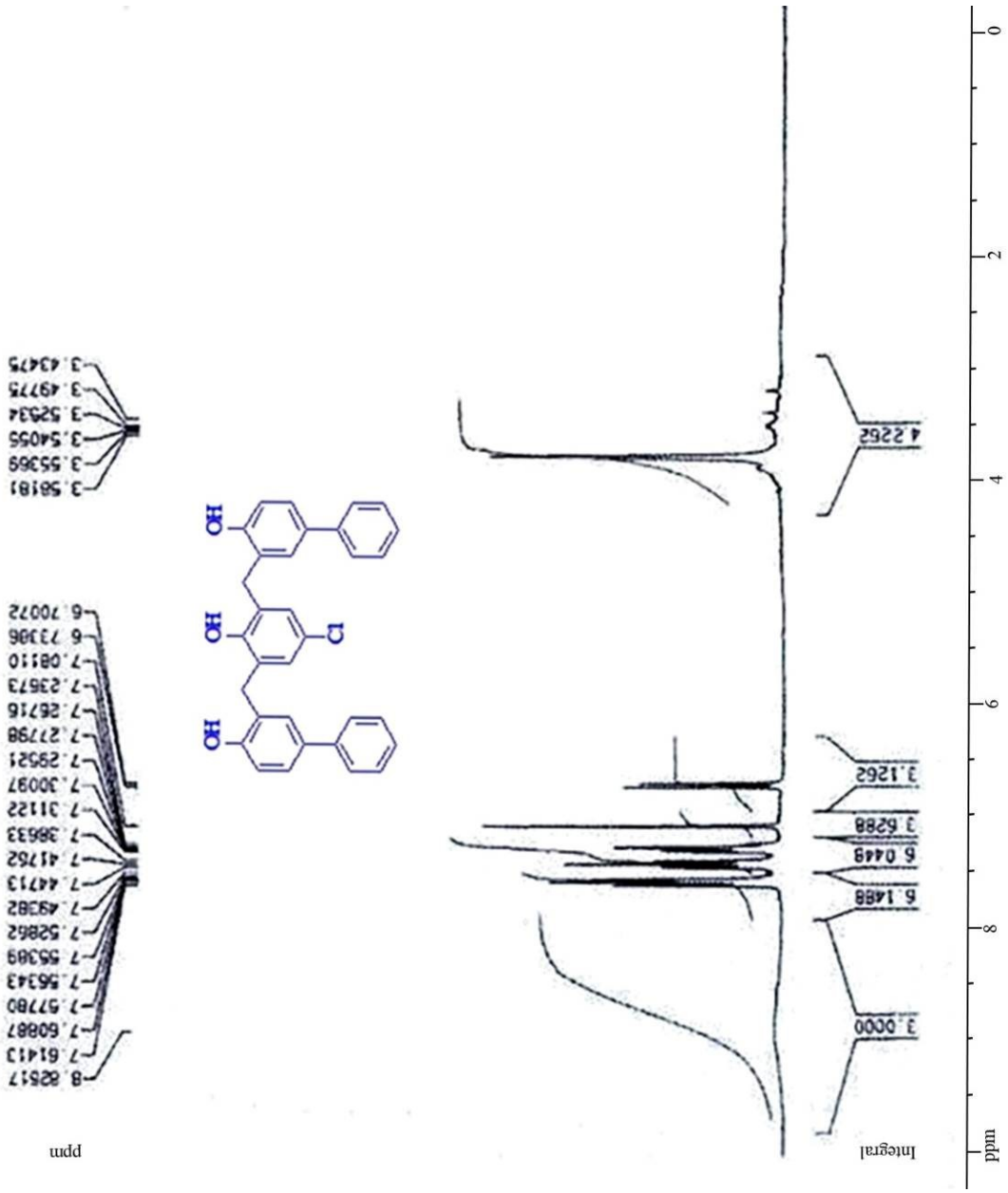

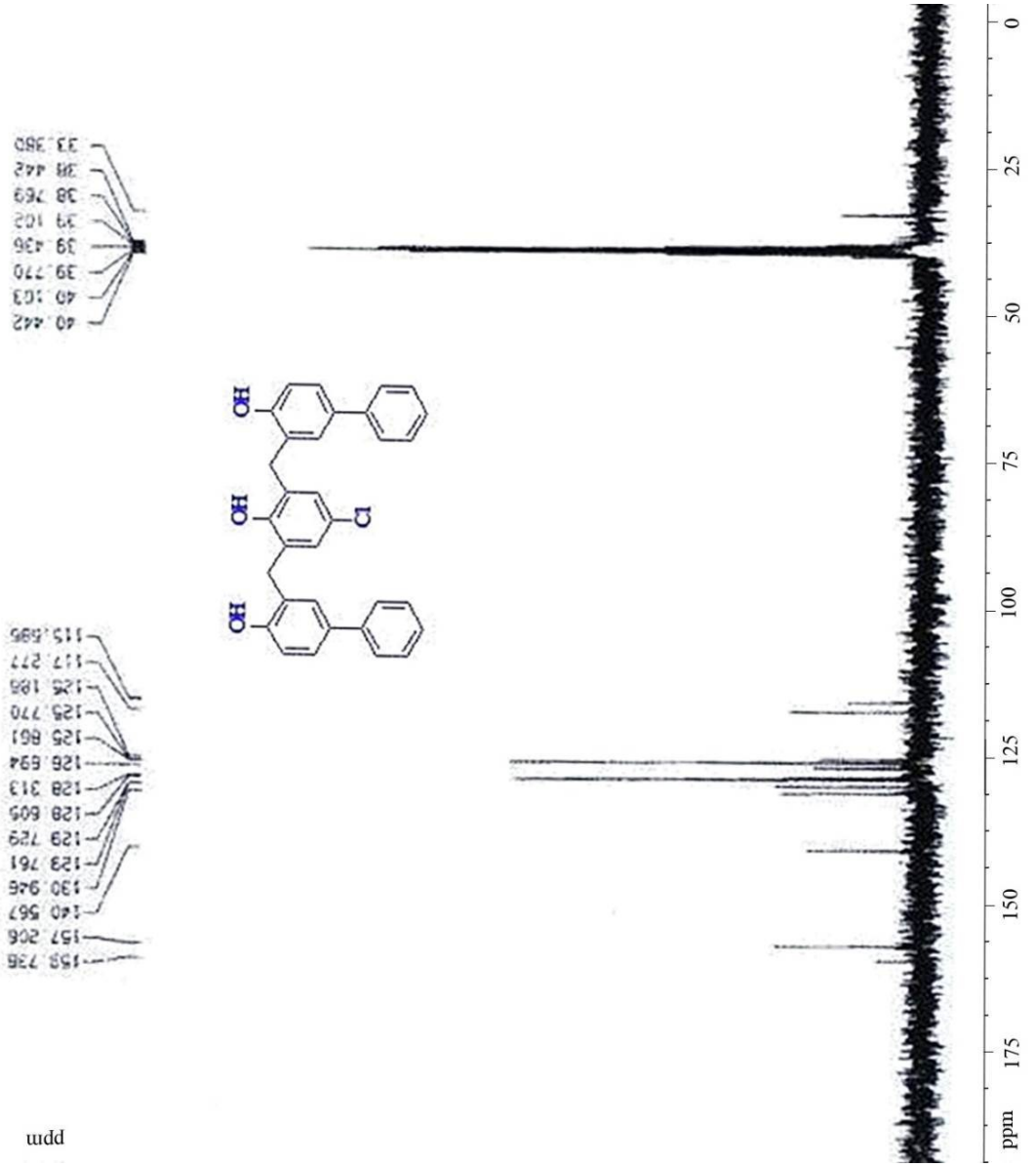
ppm
0
25
50
75
100
125
150
175
OH
OH
Cl
OH

6,6′-[(5-Chloro-2-hydroxy-1,3-phenylene)bis(methylene)]bis(4-allyl-2-methoxyphenol) (Compound C17)

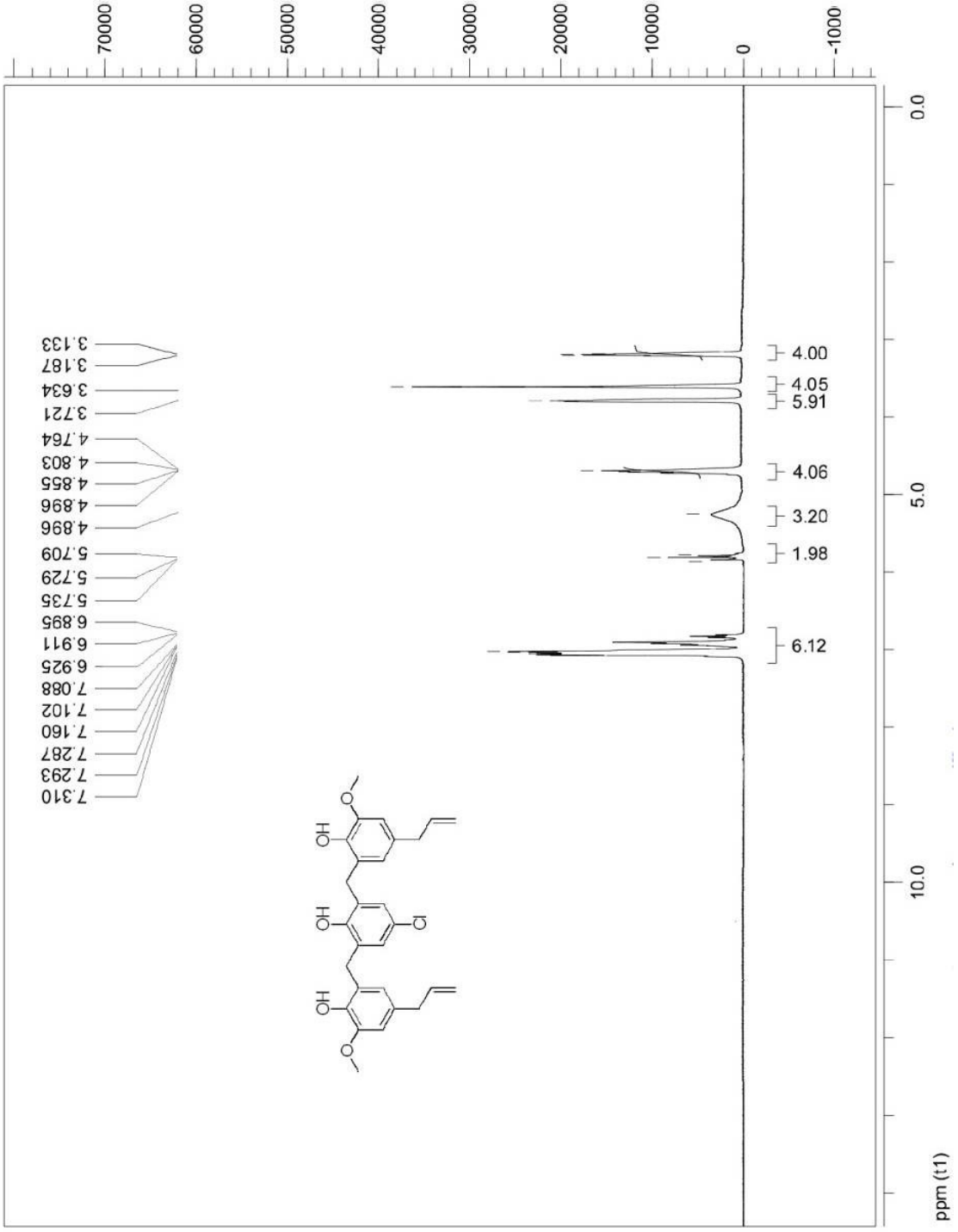

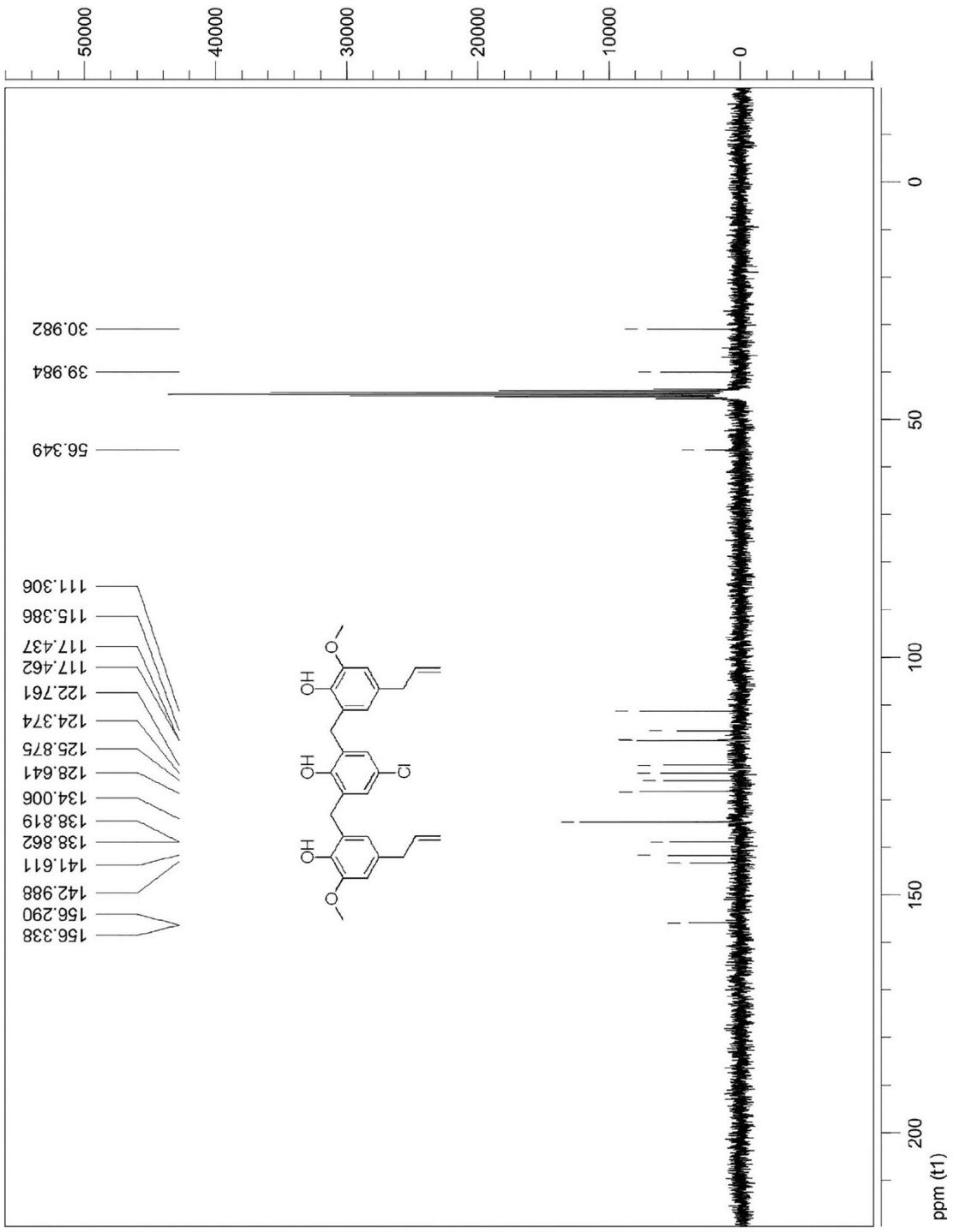
50000
40000
30000
20000
10000
0
30.982
39.984
56.349
111.306
115.386
117.437
117.462
122.761
124.374
125.875
128.641
134.006
138.819
138.862
141.611
142.988
156.290
156.338
OH
OH
OH
Cl
O
O
0
50
100
150
200
ppm (t1)

6,6′-[(5-Bromo-2-hydroxy-1,3-phenylene)bis(methylene)]bis(4-allyl-2-methoxyphenol) (Compound C18)

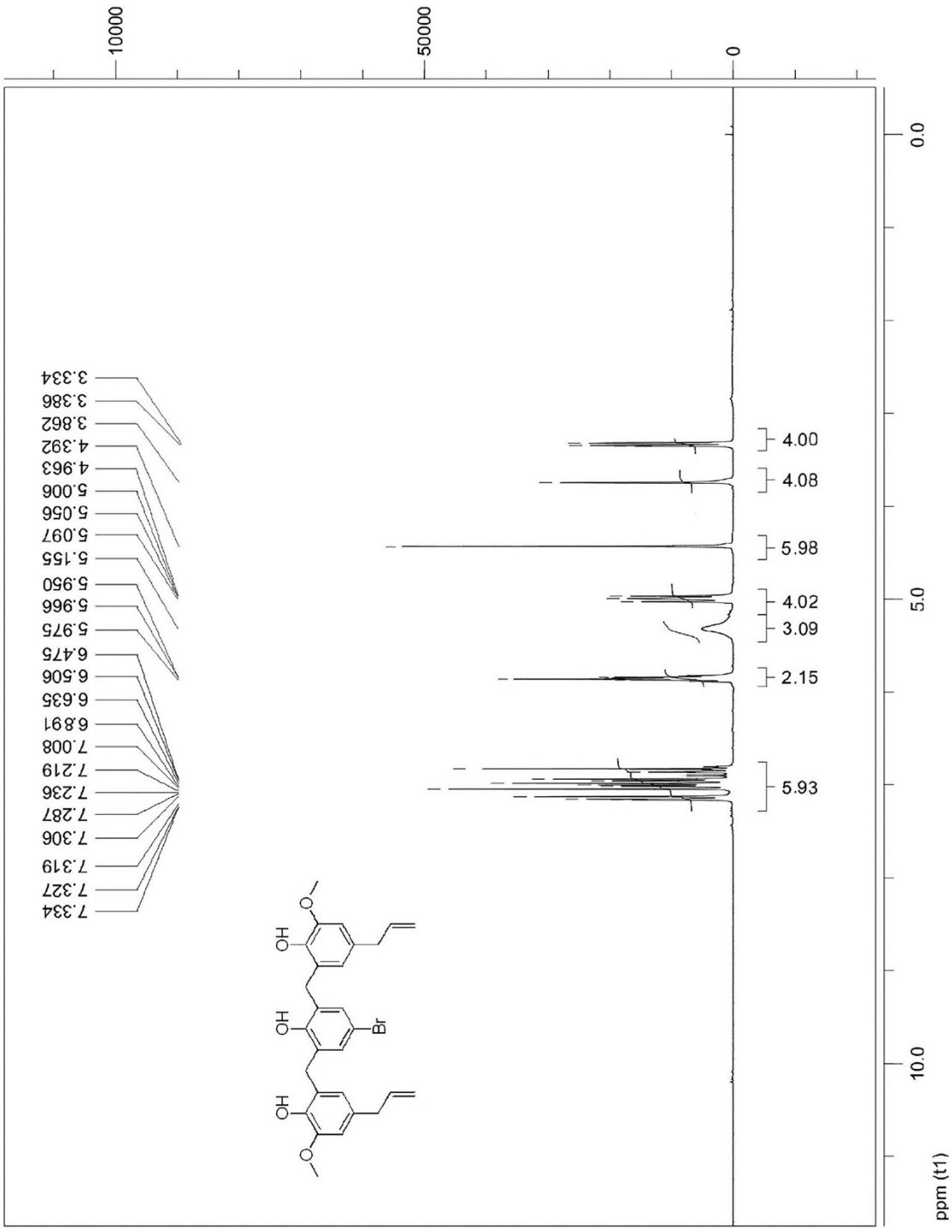

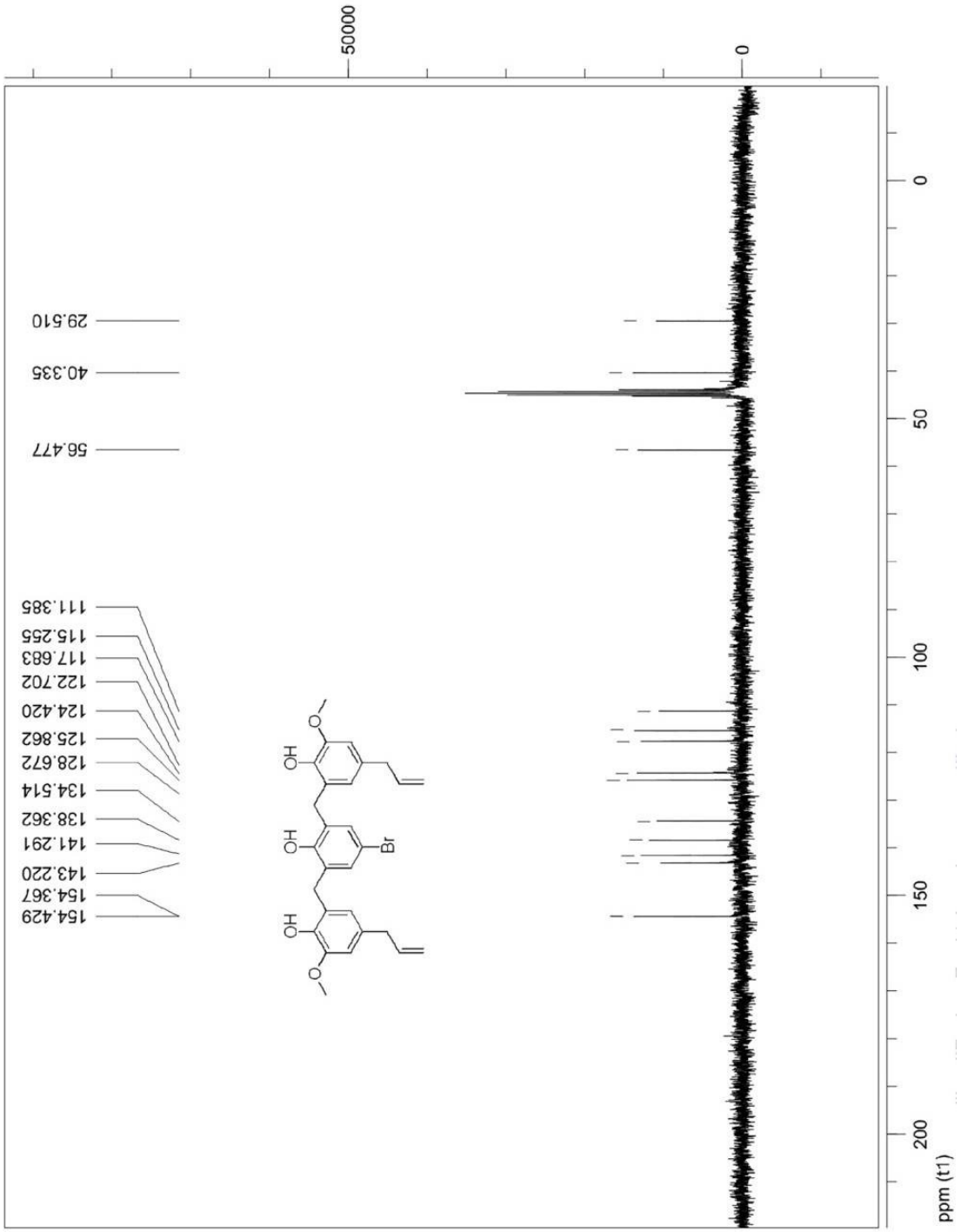
50000
0
29.510
40.335
56.477
111.385
115.255
117.683
122.702
124.420
125.862
128.672
134.514
138.362
141.291
143.220
154.367
154.429
OH
OH
OH
Br
O
O
0
50
100
150
200
ppm (t1)

1,1′-{[(5-Fluoro-2-hydroxy-1,3-phenylene)bis(methylene)]bis(5-fluoro-2-hydroxy-3,1-phenylene)}bis(ethan-1-one) (Compound C19)

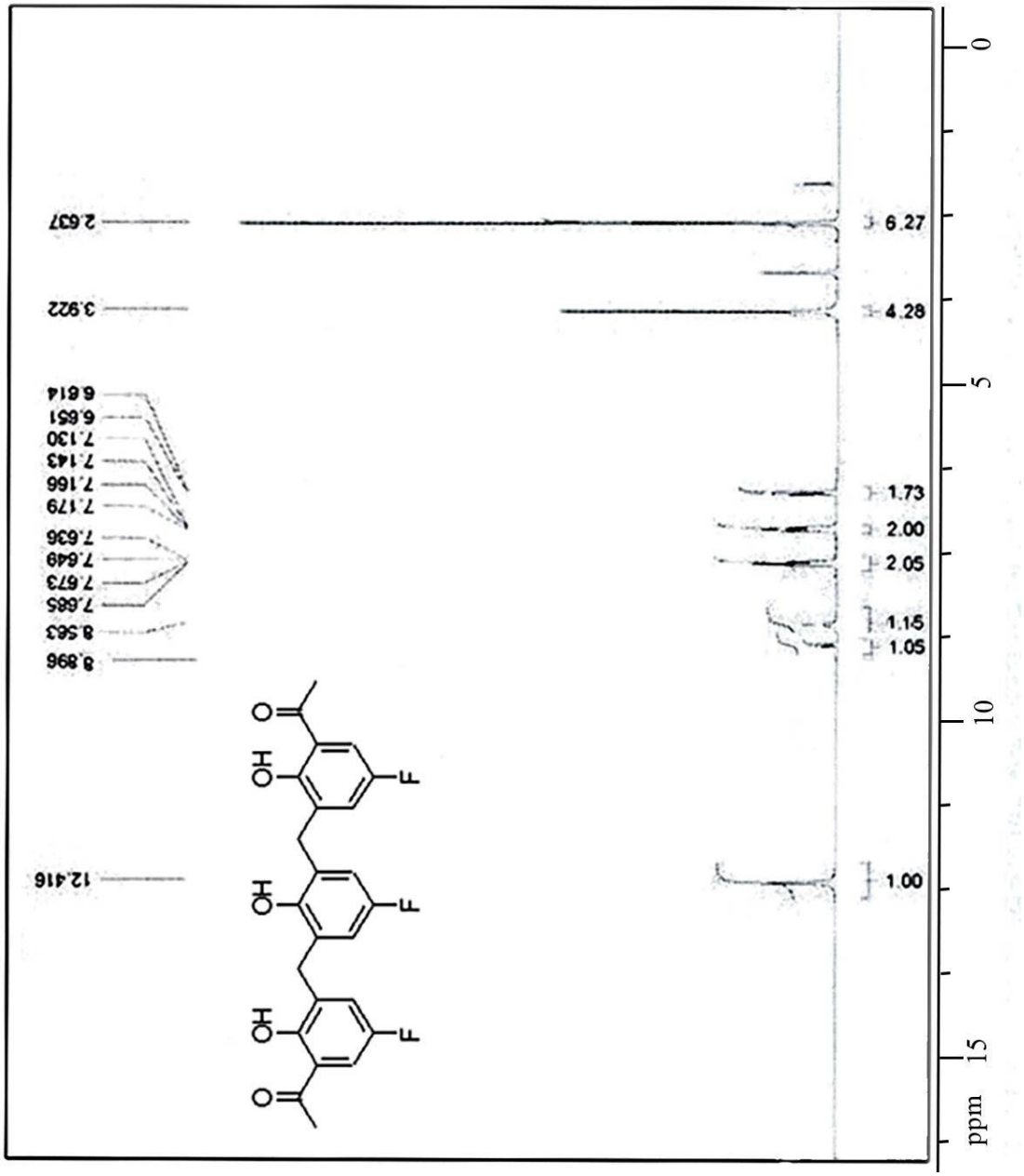

205.232
205.192
155.733
151.941
148.873
148.842
130.715
130.604
128.781
128.583
128.464
127.514
123.940
123.557
118.739
118.627
114.662
114.354
114.295
113.990
40.396
40.067
39.735
39.402
39.067
38.733
38.397
29.321
27.114
OH
F
O
ppm
0
50
100
150
200

6,6′-[(5-Chloro-2-hydroxy-1,3-phenylene)bis(methylene)]bis(2-*tert*-butyl-4-methylphenol) (Compound C20)

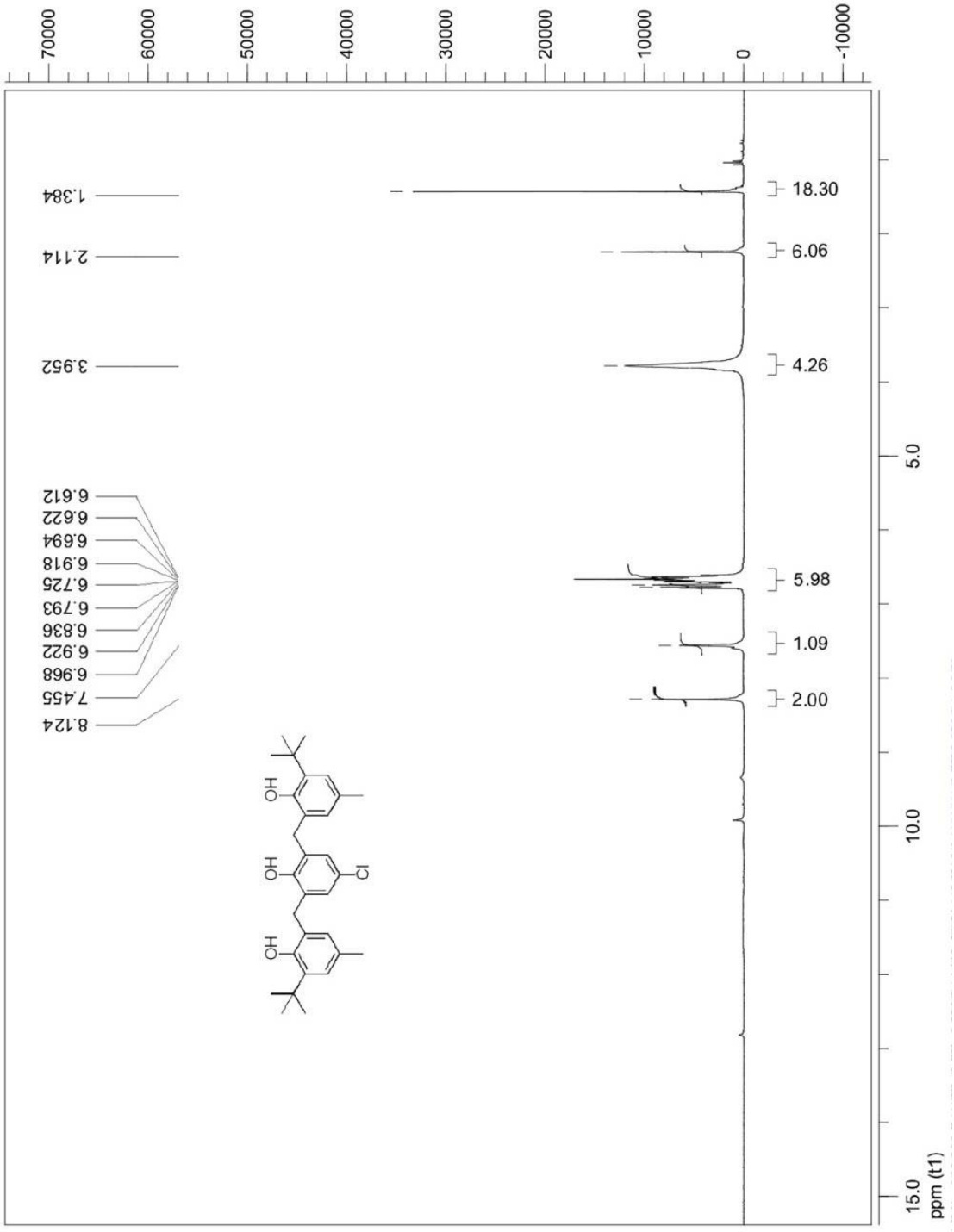

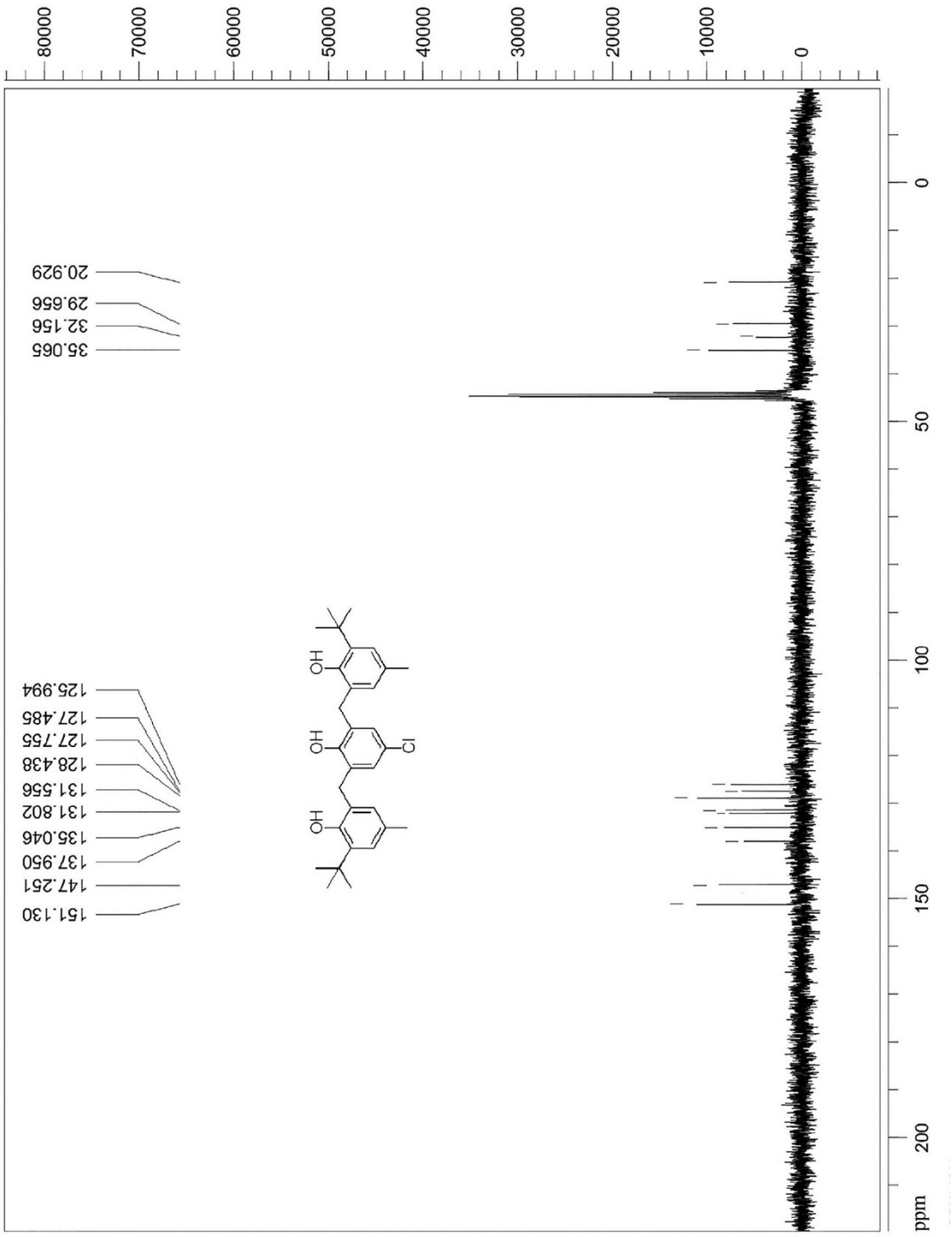
80000
70000
60000
50000
40000
30000
20000
10000
0
0
50
100
150
200
ppm
20.929
29.656
32.156
35.065
125.994
127.485
127.755
128.438
131.556
131.802
135.046
137.950
147.251
151.130
OH
OH
OH
Cl

2,6-Bis-(2-hydroxy-5-*tert*-butylbenzyl)-4-*tert*-butylphenol (Compound C21)

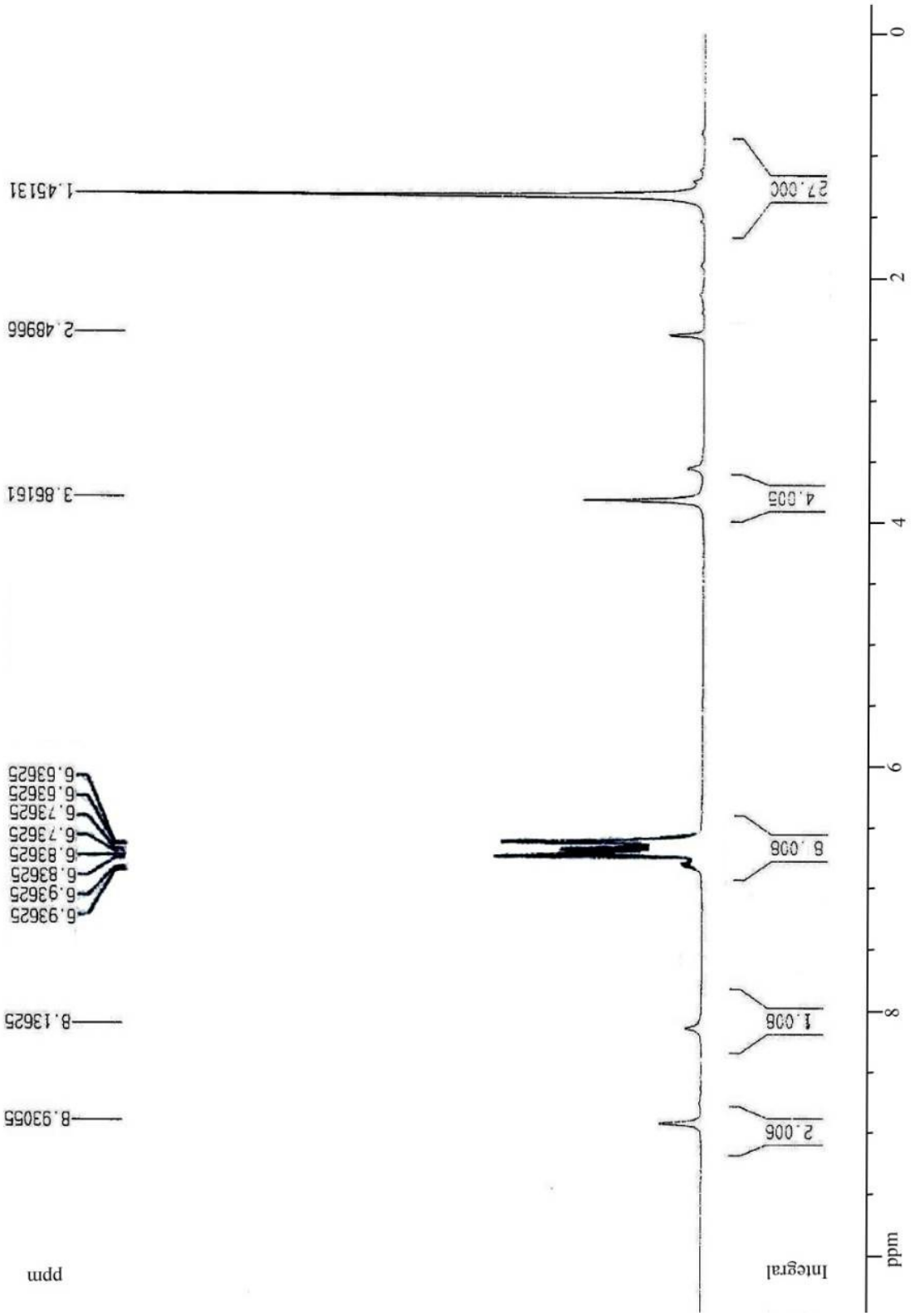

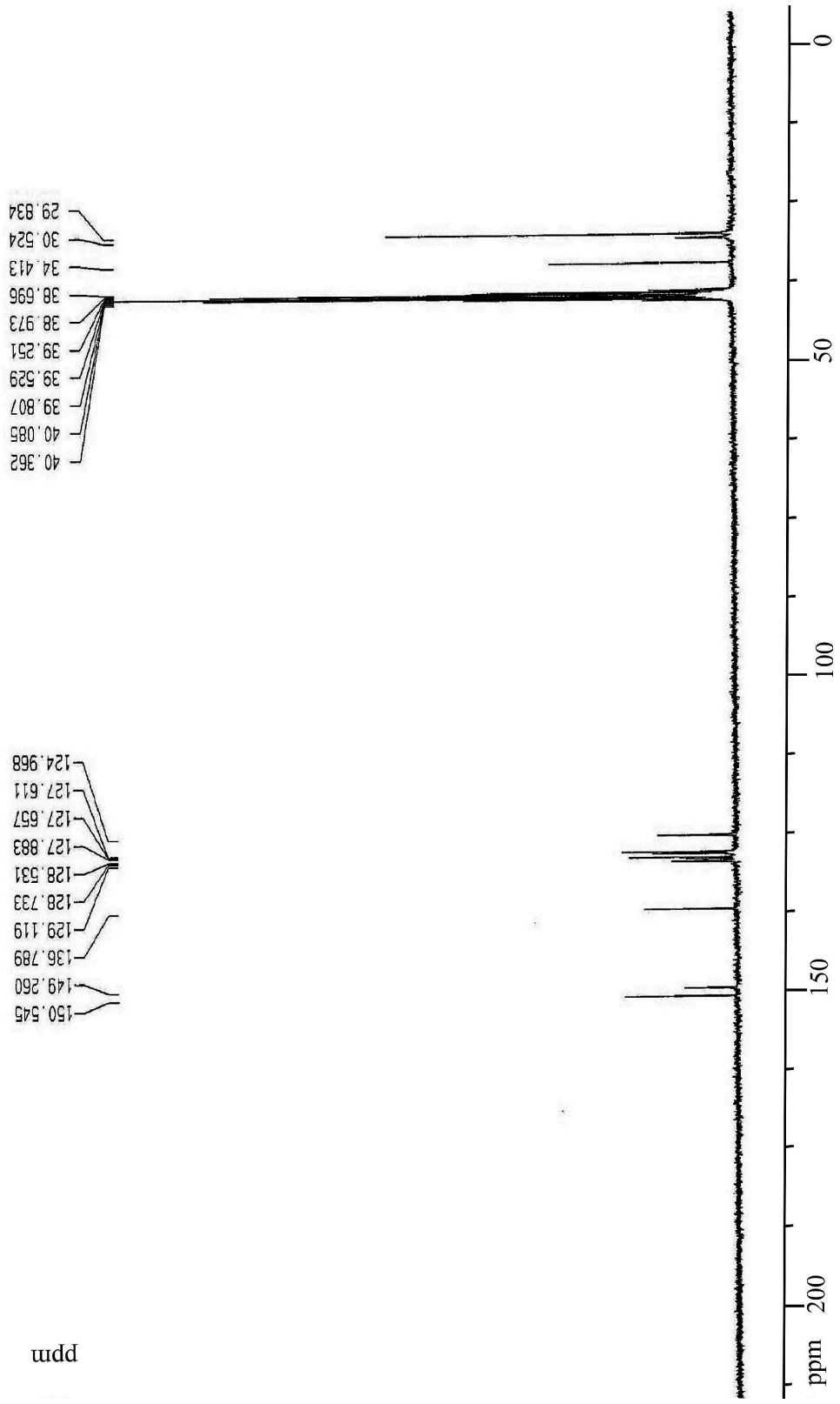

Copy of ^{1}H NMR and ^{13}C NMR of calix[4]arene derivatives

5,11,17,23-Tetramethylcalix[4]arene-25,26,27,28-tetraol (Compound D1)

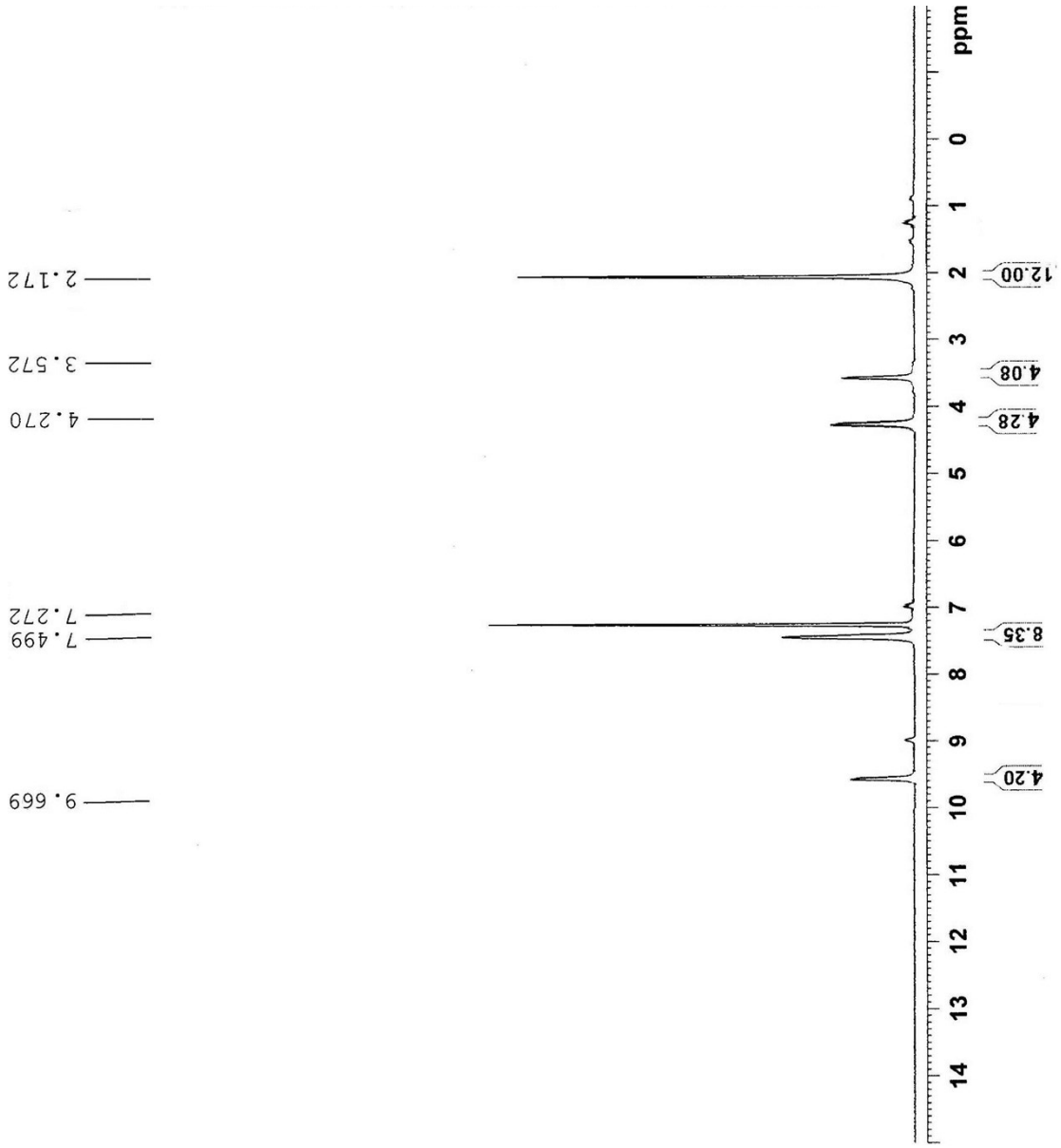

ppm
20
40
60
80
100
120
140
160
180
200
220
240
33.17
34.12
34.12
36.41
76.76
77.08
77.40
128.4
128.9
130.6
141.8
148.0
148.6

Calix[4]arene-25,26,27,28-tetraol (Compound D2)

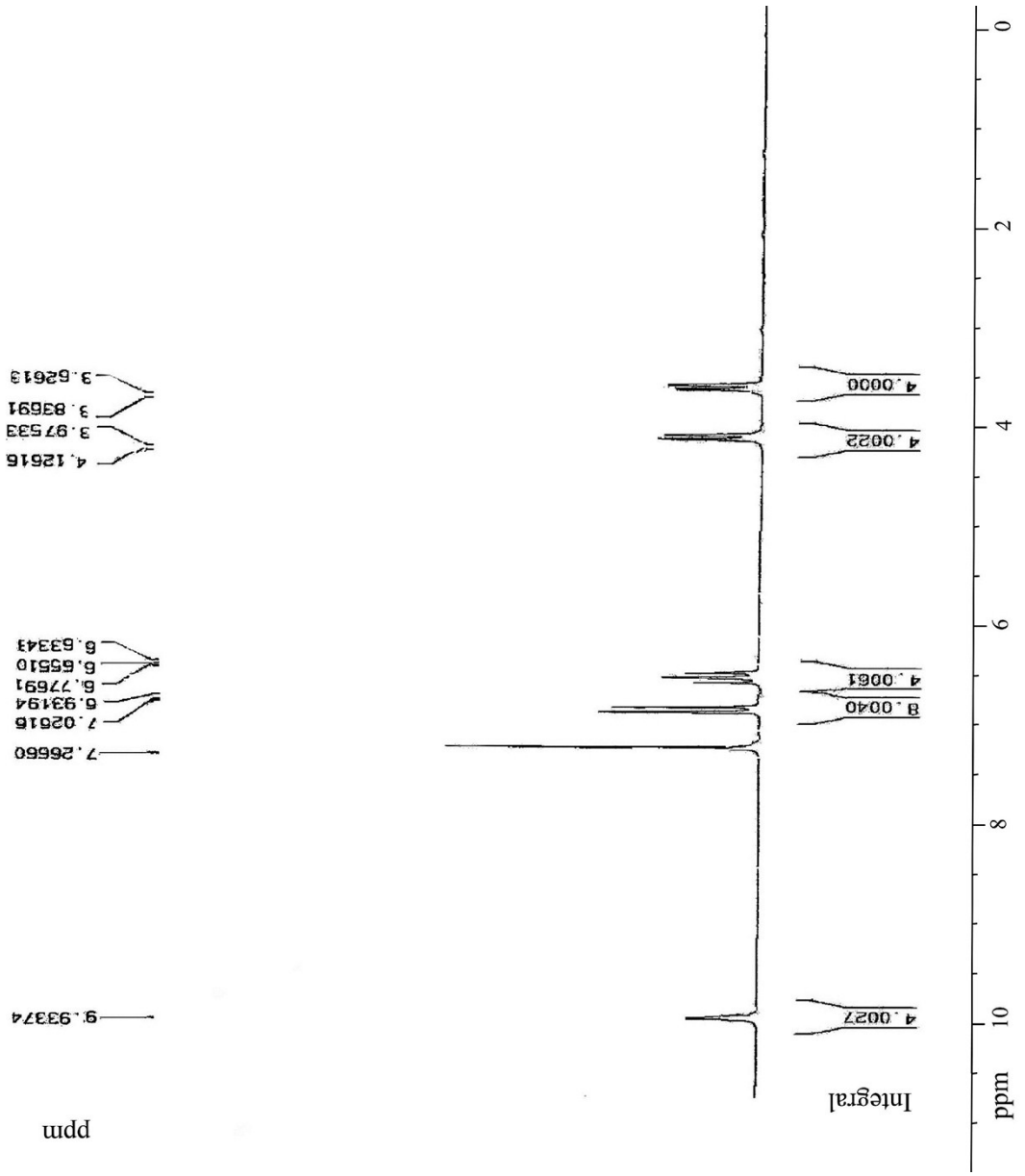

ppm
200
150
100
50
0
34.628
76.623
77.047
77.249
77.470
79.157
127.002
134.393
136.306
138.387

5,17-Dichloro-11,23-dimethylcalix[4]arene-25,26,27,28-tetraol (Compound D3)

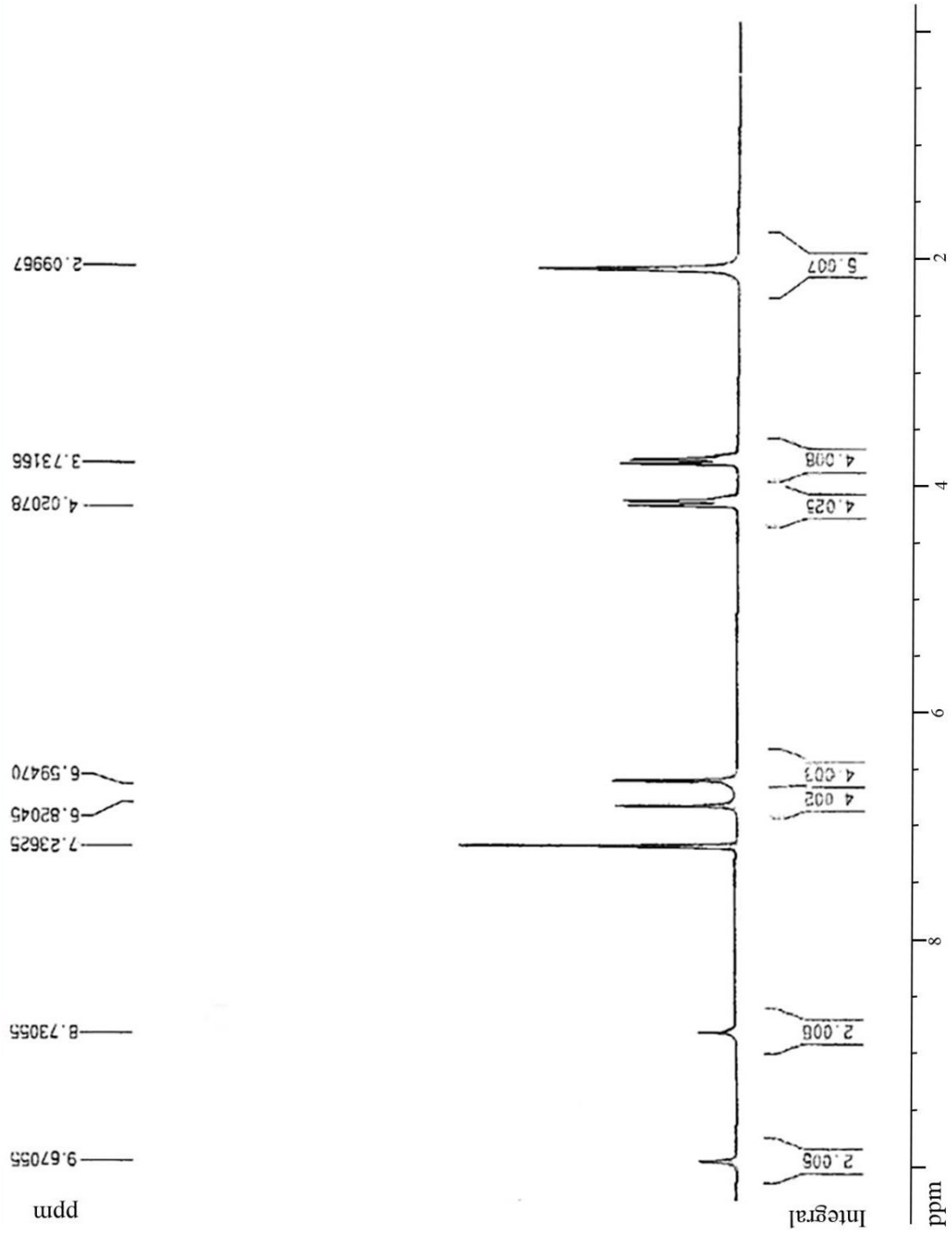

ppm
0
50
100
150
200
27.536
37.389
76.659
77.084
77.506
119.305
121.232
127.514
129.161
130.157
132.685
137.005
141.661

5,17-Dichloro-11,23-dihydroxycalix[4]arene-25,26,27,28-tetraol (Compound D4)

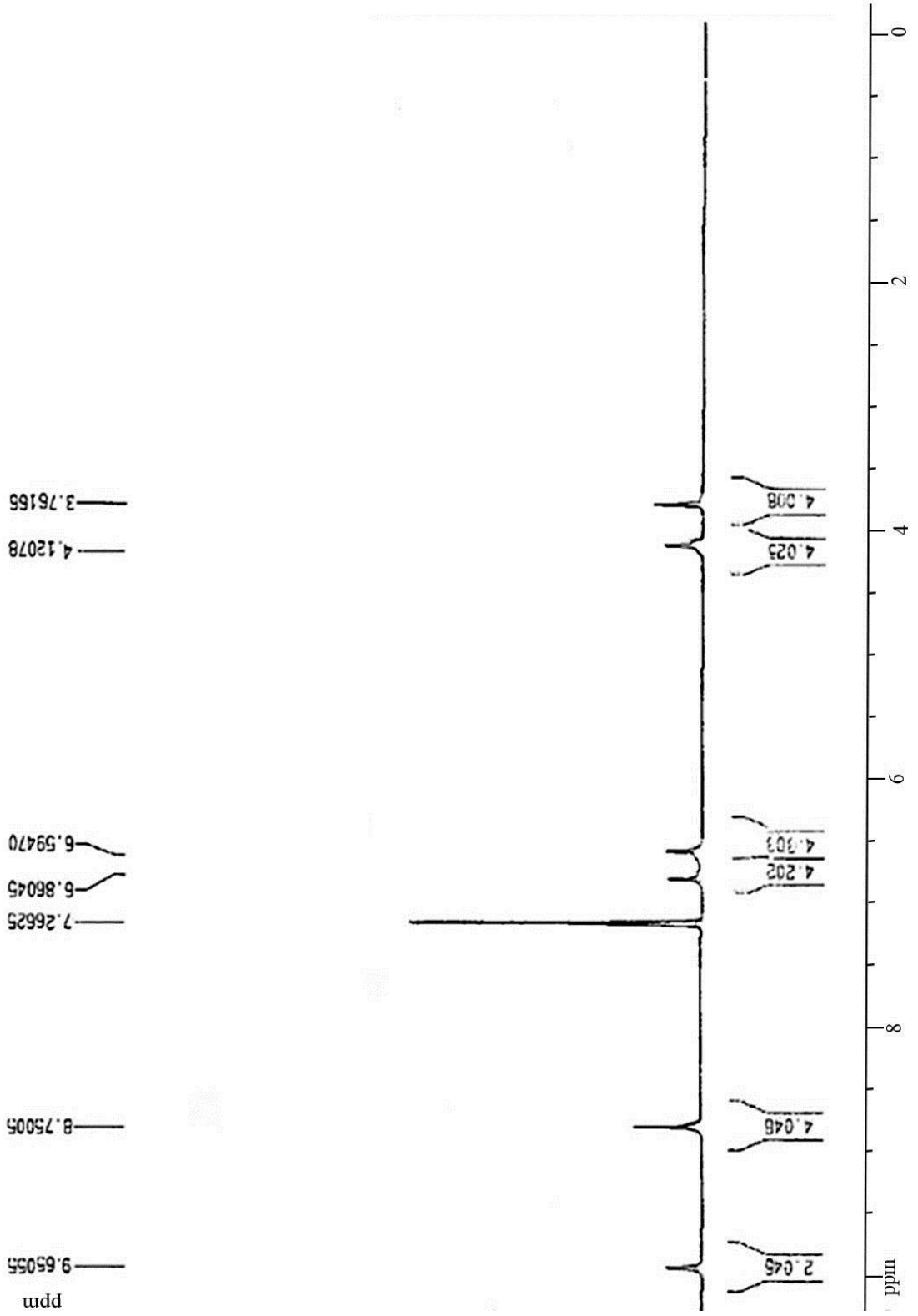

ppm
200
150
100
50
0
27.536
76.659
77.084
77.506
119.302
121.232
127.524
129.161
130.257
133.685
136.905
142.661

5,11,17,23-Tetra-*tert*-butylcalix[4]arene-25,26,27,28-tetraol (Compound D5)

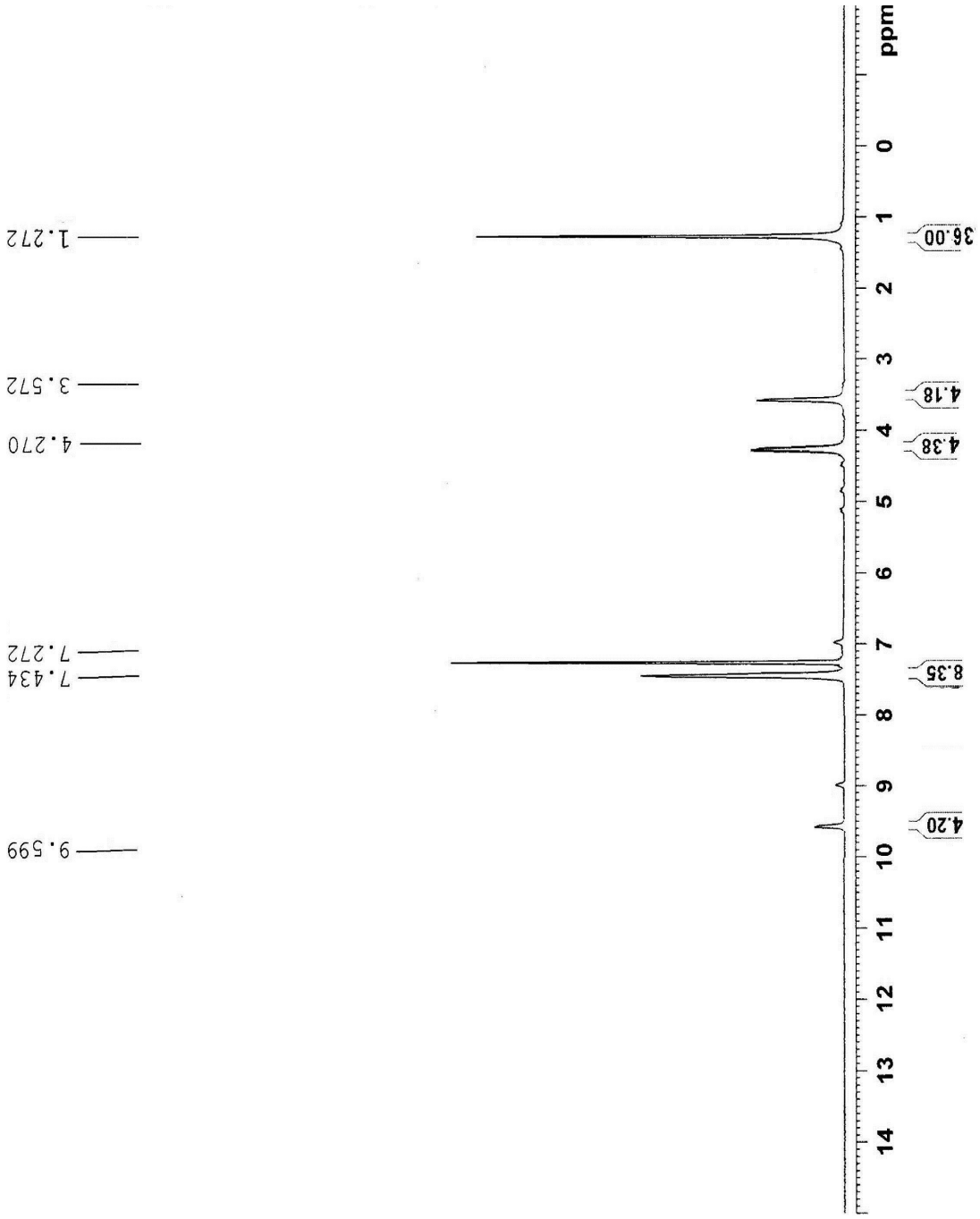

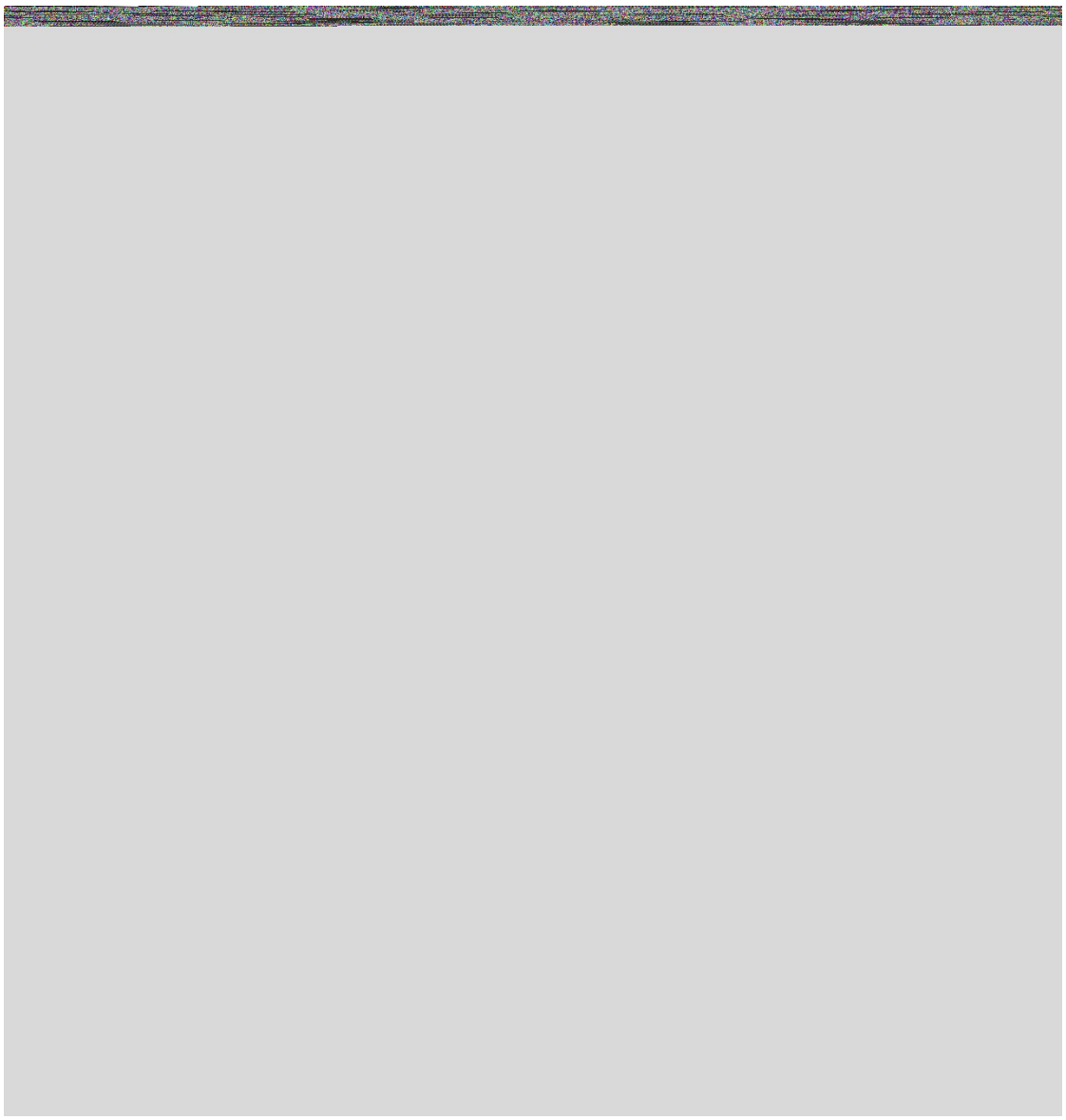

References

[1] Khalafi-Nezhad, A.; Soltani Rad, M. N.; Hakimelahi, G. H. *Helv. Chim. Acta* **2003**, *86*, 2396–2403.

[2] Khalafi-Nezhad, A.; Parhami, A.; Bargebid, R.; Molazade, S.; Zare, A.; Foroughi, H. *Mol. Divers.* **2011**, *15*, 373–381.

[3] Foster, H. M.; Hein, D. W. *J. Org. Chem.* **1961**, *26*, 2539–2541.

[4] McGarry E J, Forsyth BA (1981) 2,6-Benzyl substituted phenols. U.S. Patent 4282390.